

# Performance Bounds for LASSO under Multiplicative LogNormal Noise: Applications to Pooled RT-PCR Testing

Richeek Das<sup>a</sup>, Aaron Jerry Ninan<sup>b</sup>, Adithya Bhaskar<sup>a</sup>, Ajit Rajwade<sup>a</sup>

<sup>a</sup>*Indian Institute of Technology Bombay, Department of Computer Science and Engineering,*

<sup>b</sup>*Indian Institute of Technology Bombay, Department of Electrical Engineering,*

---

## Abstract

Group/Pooled testing is a technique which involves testing  $n$  samples for a rare disease in an indirect manner: instead of individually testing each of the  $p$  samples, it involves creating  $n < p$  pools and testing each pool, where a pool consists of a mixture of small, equal portions of a subset of the  $p$  samples. Group testing is known to save a large amount of testing time and resources in a variety of application settings. There also exist good theoretical guarantees for the recovery of the status of the  $p$  samples from results on  $n$  pools, if certain conditions are satisfied. The popularity of group testing for RT-PCR testing is also well-known. The noise in quantitative RT-PCR is known to follow a multiplicative and data-dependent model, which emerges from properties inherent to RT-PCR. In recent literature, the corresponding linear systems for inference of the health status of  $p$  samples from results on  $n$  pools, have been solved using the well-known LASSO estimator and its variants [1], which have been widely used in the compressed sensing literature. However, the LASSO has typically been used in additive Gaussian noise settings. There is no existing literature which establishes performance bounds for LASSO for the multiplicative noise model associated with RT-PCR. After noting that a general technique proposed in [2] works well for establishing performance bounds for LASSO in Poisson inverse problems, we adapt it to handle sparse signal reconstruction from compressive measurements with multiplicative noise, as would appear in pooled RT-PCR testing. In particular, we present high probability performance bounds and data-dependent weights for the LASSO and a weighted version of the LASSO under multiplicative lognormal Noise. We also show numerical results on simulated pooled RT-PCR data to

empirically validate our developed bounds.

*Keywords:* Compressed sensing, Performance Analysis and Bounds, Multiplicative Noise, Group Testing, RT-PCR

---

## 1. Introduction

The COVID-19 pandemic led to massive lockdowns worldwide, causing disruptions in industry, education and the well-being of people. Symptoms of this virus were often similar to those of the common cold, flu, etc. This, combined with the highly infectious nature of COVID-19, made early detection of the virus in individuals for subsequent isolation, one of the significant challenges faced by testing laboratories.

RT-PCR (Reverse Transcription-Polymerase Chain Reaction) [3] is a highly reliable method for detecting viruses, and was widely deployed during the COVID-19 pandemic. It involves obtaining a sample from the nose or throat of a person, chemically treating it to extract viral RNA (if present in the sample), and then converting the RNA to DNA through a process called reverse transcription. Short DNA fragments complementary to the viral DNA are added to the sample, which is then passed through a DNA amplification process. The presence of the virus is detected using fluorescent markers, and if the total fluorescence exceeds a certain threshold, the sample is considered positive for the virus. The number of cycles of amplification  $C_t$  (cycle threshold) required to exceed this threshold is reported. A larger viral load will produce a larger amount of complementary DNA and thus produce the critical level of fluorescence earlier on in the RT-PCR process, leading to a lower  $C_t$  value. Likewise, smaller viral loads are associated with higher  $C_t$  values.

However, the low prevalence rate of COVID-19 means that most test samples turn out to be negative, leading to wastage of valuable resources, if every sample has to be tested. In an effort to reduce the cost and burden of RT-PCR testing, various algorithms have been proposed, that allow for the pooling of samples in order to achieve the same or slightly lower diagnostic

---

*Email addresses:* [richeek@cse.iitb.ac.in](mailto:richeek@cse.iitb.ac.in) (Richeek Das),  
[aaronjerry12@gmail.com](mailto:aaronjerry12@gmail.com) (Aaron Jerry Ninan), [adithyabhaskar@cse.iitb.ac.in](mailto:adithyabhaskar@cse.iitb.ac.in)  
(Adithya Bhaskar), [ajitvr@cse.iitb.ac.in](mailto:ajitvr@cse.iitb.ac.in) (Ajit Rajwade)

accuracy with fewer tests [4]. One such algorithm is Tapestry, which was introduced in [1], and which combines ideas from combinatorial group testing and compressed sensing (CS). Other methods such as [5, 6] also use interesting ideas from group testing (GT) and CS. Another approach, described in [7, 8], uses additional *side information* such as family membership or via contact tracing information. This additional information is shown to further improve the accuracy of the detection algorithms. All these algorithms serve two purposes: (i) To reduce the number of testing kits required per person (which were scarce in many countries during COVID-19 surges), and (ii) To increase testing throughput by parallelizing multiple pooled tests.

Simple two-round group testing schemes such as Dorfman testing [9] had already been applied in the field by several research labs [10], [11] for COVID-19 testing. However Dorfman testing is a two-round procedure where the output of the first round acts as input to the second round. This increases testing time significantly, because the second round cannot begin before completion of the first round, and because one round of RT-PCR takes about 3-4 hours to complete. On the other hand, methods such as Tapestry [1] are non-adaptive and work in a single round. This saves on testing time, which is very critical during the peak of a pandemic. In fact, some recent research [12] argues that testing time is even more important than accuracy at the peak of a pandemic. Tapestry is based on principles of CS. CS [13] is a mathematical framework that allows for the efficient recovery of sparse signals from a small number of carefully chosen linear measurements. Let  $\mathbf{x}^* \in \mathbb{R}^p$  be a signal with only  $s \ll p$  non-zero elements at unknown indices. The signal  $\mathbf{x}^*$  is observed in an indirect manner via linear measurements of the form  $\mathbf{y} = \mathbf{A}\mathbf{x}^* + \mathbf{w}$  where  $\mathbf{A} \in \mathbb{R}^{n \times p}$ ,  $n \ll p$  is a so called sensing matrix with fewer rows than columns,  $\mathbf{y} \in \mathbb{R}^n$  is a measurement vector, and  $\mathbf{w} \in \mathbb{R}^n$  is an additive noise vector. Using simple convex optimization procedures, it has been shown that the sparse vector  $\mathbf{x}^*$  can be recovered stably and robustly from  $\mathbf{y}$ ,  $\mathbf{A}$  provided two (related) conditions are met: (i) The number of measurements should be at least  $O(s \ln p)$ , and (ii) The matrix  $\mathbf{A}$  should obey the property that its nullspace accommodates no signal with  $s$  or fewer than  $s$  non-zero elements, barring the zero vector. CS has found numerous applications in signal processing, image reconstruction, and other fields and has been particularly useful for sparse linear inverse problems, such as those encountered in pooled RT-PCR testing. Note that most traditional GT algorithms (see [14] for a survey) treat both  $\mathbf{y}$  and  $\mathbf{x}^*$  as binary. However, CS produces a distinct advantage over these traditional GT algorithms: it allows

us to determine *quantitative* information such as viral load, over and above a mere binary indicator of whether or not the sample is diseased [5, 1, 7, 8].

The well known LASSO estimator in statistics [15] and its variants are popular methods for solving sparse linear inverse problems in CS. The estimator is given as follows:

$$\hat{\mathbf{x}} := \operatorname{argmin}_{\mathbf{x}} \|\mathbf{y} - \mathbf{A}\mathbf{x}\|^2 + \lambda \|\mathbf{x}\|_1, \quad (1)$$

where  $\lambda > 0$  is a regularization parameter. LASSO has been used in group testing, including the Tapestry algorithm [1]. Its variants such as the group LASSO [16] are useful methods to exploit *side information* to enhance group testing performance [7, 8]. There is a rich literature on theoretical performance bounds for the LASSO under additive Gaussian [15, Chapter 11] and Poisson noise [2, 17]. [2] also provides a novel analysis of a *weighted* version of LASSO, deriving data-dependent weights and chalking out a generalized framework for handling data-dependent noise, with emphasis on the Poisson noise model which is widely used for optical imaging systems. However, the nature of RT-PCR testing introduces multiplicative noise (as we shall see in detail in Sec. 2.1), whose effective variance scales directly with the values of the unknown vector  $\mathbf{x}^*$ . While the LASSO has been shown to numerically perform well in this setting [1], its theoretical bounds for this noise model have not been established in the literature to the best of our knowledge. It is important to have a better understanding of the theoretical performance guarantees of the LASSO under multiplicative noise to rigorously justify the use of this estimator in a multiplicative noise setting such as that encountered in pooled RT-PCR.

In this paper, we draw from a general technique proposed in [18] and adapt the data-dependent performance bounds for LASSO in Poisson inverse problems as presented in [2], to the case of multiplicative noise in the context of pooled RT-PCR testing. We derive high-probability performance bounds, obtained via data-dependent weights for LASSO and its weighted variant (details provided later in this paper), assuming randomly generated Bernoulli pooling matrices. We support our theory through numerical experiments.

In parallel to this work, our group has done other work [19] on the analysis of the LASSO for multiplicative noise in compressive RT-PCR. This work may be submitted for publication later, independent of the work presented in this paper. There are two main differences between [19] and this work: (*i*) the former does not explore a weighted version of LASSO, as we do here

(see Equation 6), and (ii) unlike [19], the work here considers a Taylor series based expansion of the multiplicative noise model (see Eqns. 2 and 3).

Lastly, we note that non-Gaussian noise has been extensively considered in many branches of signal processing. Poisson noise is considered in compressed sensing in [20, 21]. Moreover, [22] deals with optimal experiment design for ARX models under non-Gaussian noise. Likewise, [23] deals with robust identification of output error models in the presence of heavy-tailed, non-Gaussian noise. On the other hand, our paper considers a very specific non-Gaussian noise model – multiplicative lognormal noise, which arises in RT-PCR. Moreover it deals with compressive recovery unlike the two aforementioned papers.

## 2. Theory

### 2.1. Problem Formulation

In RT-PCR testing, a naso- or oro-pharyngeal swab is taken from a person being tested. The mucus in the swab is mixed in a liquid medium and tested in an RT-PCR machine. [24] surveys multiple group testing techniques in detail, where they pool (mix) subsets of  $p$  samples and test the  $n$  pools ( $\#\text{pools}(n) < \#\text{samples}(p)$ ) to save resources. Small, equal portions of participating samples are used for creating any pool. Given a negative pooled test, one can conclude that all contributing samples are non-infected, as RT-PCR is known to be highly sensitive by design due to the DNA amplification involved. In case some of the pooled tests are positive, we would like to deduce which participants are infected without repeated rounds of testing. This part is non-trivial.

More formally, we can state the computational problem as follows. Let  $\mathbf{x}^* \in \mathbb{R}^p$  represent the vector of viral loads of the samples collected from  $p$  individuals (one per individual). All entries of  $\mathbf{x}^*$  are non-negative and  $x_i = 0$  would imply that the sample of the  $i$ th individual is not infected. To model the low infection rate for COVID-19, we consider  $\mathbf{x}^*$  to be a sparse vector with very few positive valued elements. The mixing of samples into groups (or pools) can be modeled with the help of a binary mixing matrix  $\mathbf{A} \in \{0, 1\}^{n \times p}$  (also called pooling matrix or sensing matrix), where  $n < p$  and where entry  $A_{ij}$  is 1 if the sample from the  $j$ th person is included while creating the  $i$ th pool and 0 otherwise. The resulting viral loads in pooled samples will be given by  $\mathbf{y} \in \mathbb{R}^n$ , where:  $y_j = \sum_{i=1}^p A_{ji}x_i^* = \mathbf{A}^j \mathbf{x}^*$ ,  $1 \leq j \leq n$ . Here,  $\mathbf{A}^j$  is the  $j$ th row of  $\mathbf{A}$ .

However, due to the stochasticity of the reaction, measurement error in the PCR machine, and exponential growth of the number of molecules of viral cDNA in all the pools, a multiplicative lognormal noise model is used for  $\mathbf{y}$ . We use the noise model derived in [1] for our analysis:

$$y_j = \mathbf{A}^j \mathbf{x}^* (1 + q_a)^{w_j}. \quad (2)$$

Here,  $q_a \in (0, 1)$  is the known fraction of viral cDNA that replicates in each cycle (sometimes referred to as the amplification factor), and  $w_j \sim \mathcal{N}(0, \sigma^2)$  is the sample of a random variable which represents the difference between the true cycle time and observed/recorded cycle time. Here  $\sigma$  is the standard deviation of  $w_j$ . Usually, the time difference is small, and hence we can assume  $\sigma < 1$  (Fig.1 of Additional File 3 in [25]), as has also been done in [1, 7].

Several classes of binary pooling matrices have shown promising results when applied to the problem of inferring  $\mathbf{x}^*$  from  $\mathbf{y}, \mathbf{A}$ , as shown in [1]. This includes different types of deterministically generated matrices. However, these typically have restrictions on the number of rows and columns as discussed in [1]. Hence, for greater flexibility, and to simplify our analysis, we limit our study to the class of random Bernoulli sensing matrices, where each element of the matrix is drawn independently from the Bernoulli( $q$ ) distribution for some  $q \in (0, 1)$ . That is, each entry  $A_{ij}$  of matrix  $\mathbf{A}$  is independently 0 with probability  $1 - q$  and 1 with probability  $q$ . Bernoulli matrices are useful for simplicity of pool creation: a sample either participates in a pool/group ( $A_{ij} = 1$ ) or it does not ( $A_{ij} = 0$ ), whereas fractional entries would make pooling much more cumbersome.

Our study is in the low variance regime, i.e.  $\sigma < 1$ , which we would later see appears to be an essential assumption for accurate or near-accurate recovery of  $\mathbf{x}^*$  from  $\mathbf{y}, \mathbf{A}$ . This assumption is also supported in practice by RT-PCR systems, since the variance of the cycle time readings is very low as mentioned earlier. Additionally, this assumption allows us to approximate the multiplicative lognormal noise model by linearizing Equation (2) using a first order Taylor series expansion, as also mentioned in [7, Sec. VII]:

$$y_j \approx \mathbf{A}^j \mathbf{x}^* + [\mathbf{A}^j \mathbf{x}^* \ln(1 + q_a)] w_j, \text{ where } w_j \sim \mathcal{N}(0, \sigma^2). \quad (3)$$

Our target is to recover vector  $\mathbf{x}^*$  using our pooled viral loads  $\mathbf{y}$  and the pooling matrix  $\mathbf{A}$ . Note that the approximation in the above equation is tight since  $\sigma < 1$ , all powers of  $\ln(1 + q_a)$  are less than 1 and due to division

by factors such as  $2!$ ,  $3!$ , etc. All this makes the second-order or higher order terms of the Taylor series expansion negligible in magnitude. The Taylor expansion of  $y_j$  is as follows:

$$y_j \approx \mathbf{A}^j \mathbf{x}^* \left( 1 + \ln(1 + q_a)w_j + \frac{1}{2} \ln^2(1 + q_a)w_j^2 + \dots \right) \quad (4)$$

As  $w_j \sim \mathcal{N}(0, \sigma^2)$  and  $\sigma < 1$ , we can ignore the higher order terms of  $w_j^2$ ,  $w_j^3$ ,  $\dots$ , and end up with Equation (3). Ideally, this approximation is valid only with high probability. But for simplicity, we treat it as exact.

The Taylor series expansion casts this model as a special case of additive signal dependent noise. Note that the additive noise variance in this model (see Equation (3)) is proportional to the *square* of the mean, unlike the case of Poisson noise, where the noise variance is *equal* to the mean. Along a related vein, the work in [26] presents an interesting case where the noise in the compressive measurements is linearly correlated with the signal, and many applications including quantization noise are handled. However no theoretical performance bounds are presented, and multiplicative noise is not considered.

## 2.2. Estimation methods

We consider two estimators in this work: the LASSO and the weighted LASSO (referred to henceforth as WLASSO), both for the case of multiplicative noise in  $\mathbf{y}$ .

The LASSO estimator is presented here below:

$$\hat{\mathbf{x}}^L = \underset{\mathbf{x} \in \mathbb{R}^p}{\operatorname{argmin}} \|\mathbf{y} - \mathbf{A}\mathbf{x}\|_2^2 + \gamma \sum_{k=1}^p \beta |x_k|, \quad (5)$$

where  $\gamma > 2$  is a constant and  $\beta > 0$  is a data-dependent scalar.

The WLASSO estimator uses a possibly different weight for each element of  $\mathbf{x}$ , as shown below:

$$\hat{\mathbf{x}}^{WL} = \underset{\mathbf{x} \in \mathbb{R}^p}{\operatorname{argmin}} \|\mathbf{y} - \mathbf{A}\mathbf{x}\|_2^2 + \gamma \sum_{k=1}^p \beta_k |x_k|, \quad (6)$$

where  $\gamma > 2$  is a constant and  $\beta_k > 0$  is the  $k$ th data-dependent scalar. The exact expressions of  $\beta$  and  $\beta_k$  depend on the observed data. Deriving

expressions for  $\beta$  and  $\beta_k$  forms the crux of our work in this paper (albeit for modified forms of these estimators presented later in Equation (12) and Equation (13)).

Additionally, note that a logarithmic transformation on  $\mathbf{y}$  will act as a variance stabilization transform [27] for multiplicative noise, just as the square-root transform acts a variance stabilizer for Poisson noise and has shown great success in Poisson/Poisson-Gaussian inverse problems [20, 21], tomography [28] and deblurring [29]. The associated estimator for our multiplicative noise outlined in Equation (2), i.e.  $\operatorname{argmin}_{\mathbf{x}} \|\ln \mathbf{y} - \ln \mathbf{A}\mathbf{x}\|_2^2 + \lambda \|\mathbf{x}\|_1$ , might seem like an obvious choice. However, we have observed that such an estimator produces very poor results in practice, and has many convergence issues. Hence, we have not pursued it further in this work. Similar observations have also been reported in [7, Sec. VII-A].

Let  $S^*$  be the support of  $\mathbf{x}^*$  (the true, unknown vector of  $p$  viral loads) having size  $s = |S^*|$ . Under this condition of exact sparsity, [18, Corollary 2] states that if the sensing matrix  $\mathbf{A}$  satisfies the so-called Restricted Eigenvalue Condition (REC, defined later) and the column normalization condition, then the optimal solution  $\hat{\mathbf{x}}^L$  of the LASSO instance, with regularization parameter  $\beta = 4\sigma\sqrt{\frac{\ln p}{n}}$ , satisfies a high probability performance bound which increases in direct proportion to the regularization parameter. However, [18] sets a requirement on  $\beta$  for this bound to hold:  $\beta \geq 2\|\nabla\mathcal{L}\|_\infty$  where  $\mathcal{L}(\cdot)$  is the likelihood function, i.e.,  $\beta$  should be greater than twice the  $l_\infty$  norm of the gradient of the quadratic loss in LASSO. This becomes particularly restrictive when we apply it to the general case of WLASSO from Equation (6), where we have a separate regularization parameter  $\beta_k$  for each element of the signal. Instead, we can extend this by lower bounding each  $\beta_k$  by the absolute value of its individual gradient term, i.e. by  $|(\mathbf{A}^T(\mathbf{y} - \mathbf{A}\mathbf{x}^*))_k|$ .

Under this new condition on  $\beta_k$ , we have the following risk bounds for the weighted and classical LASSO estimates ( $\hat{\mathbf{x}}^{WL}$  and  $\hat{\mathbf{x}}^L$  respectively) when  $\mathbf{A}$  and  $\mathbf{y}$  follow the conditions of Proposition 3 outlined later in the paper. Here  $\rho_\gamma$  only depends on  $\gamma$  and  $\eta$  is a parameter associated with the restricted eigenvalue condition (REC) of the sensing matrix  $\mathbf{A}$ :

$$\|\hat{\mathbf{x}}^{WL} - \mathbf{x}^*\|_2^2 \leq \frac{\rho_\gamma^2}{\eta} \sum_{k \in S^*} \beta_k^2; \quad \|\hat{\mathbf{x}}^L - \mathbf{x}^*\|_2^2 \leq \frac{\rho_\gamma^2}{\eta} s\beta^2. \quad (7)$$

Looser bounds than those shown here can be obtained from an analysis of the WLASSO estimator using the typical LASSO bounding procedures outlined in



[18]. Following from the prior discussion, if each  $\beta_k$  in the WLESSO estimator is close to  $|(\mathbf{A}^T(\mathbf{y} - \mathbf{A}\mathbf{x}^*))_k|$ , then the bounds on the WLESSO are close to those of the oracle least squares estimator [18, 2]. But practically, we cannot set  $\beta_k$  to these values as the weights should only depend on the observed data. However, we can still obtain reasonable estimates of these weights based on the characteristics of the data, as we do in this work.

$$\text{Condition } \mathcal{C}1 \text{ on } (\{\beta_k\}_k) : |(\mathbf{A}^T(\mathbf{y} - \mathbf{A}\mathbf{x}^*))_k| \leq \beta_k \quad \forall k = 1, \dots, p. \quad (8)$$

We want the *smallest* possible values of  $\beta_k$  which would faithfully satisfy the Condition  $\mathcal{C}1$  with high probability. This serves as our primary objective in deriving the data-dependent weights for our noise model as stated in Section 2.3.

### 2.3. Assumptions and Data-Dependent Weights

Here we present the data-dependent weights and the underlying assumptions we propose for the LASSO and WLESSO estimators defined in Equation 5 and Equation 6, respectively. In this section, we outline the overall approach and a broad proof sketch, while a full proof for these expressions can be found in the Supplemental Material. We further demonstrate simulation results in Section 3, and theoretical performance bounds in Section 2.4 using these weights.

We first impose a condition on the sensing matrix required for reconstruction using the variants of the LASSO estimator. This is known as the *Restricted Eigenvalue Condition*. It is defined below here, following [15, Chapter 11]: A sensing matrix  $\mathbf{A}$  of size  $n \times p$  is said to obey the Restricted Eigenvalue Condition (REC), if there exist constants  $\kappa_1, \kappa_2 > 0$  such that

$$\|\mathbf{A}\mathbf{x}\|_2 \geq \kappa_2\|\mathbf{x}\|_2 - \kappa_1\|\mathbf{x}\|_1, \quad \forall \mathbf{x} \in \mathbb{R}^p. \quad (9)$$

#### 2.3.1. Rescaling and Recentering

The random Bernoulli sensing matrix which is suitable for pooled testing does not obey the REC. Instead, we define a surrogate pooling matrix  $\tilde{\mathbf{A}}$  which would obey the REC and a surrogate measurement vector  $\tilde{\mathbf{y}}$ . We want a complementary transformation to generate  $\tilde{\mathbf{y}}, \tilde{\mathbf{A}}$  from  $\mathbf{y}, \mathbf{A}$ . Ideally, we want the Gram matrix of our surrogate pooling matrix to be as homogeneous as possible. We invoke the following two commonly used conditions to obtain our surrogate matrices:

$$\mathbb{E} \left( \tilde{\mathbf{A}}^T \tilde{\mathbf{A}} \right) = \mathbf{I}_p; \mathbb{E} \left( \tilde{\mathbf{A}}^T \left( \tilde{\mathbf{y}} - \tilde{\mathbf{A}}\mathbf{x}^* \right) \right) = \mathbf{0}. \quad (10)$$

In Equation (10),  $\mathbf{I}_p$  stands for a  $p \times p$  identity matrix. The first constraint in Equation (10) helps us ensure that the REC defined in Equation (9) holds. We impose the second constraint in Equation (10) to make  $\beta_k$  as small as possible, while satisfying the Condition  $\mathcal{C}1$ . Based on the calculations in [2, Appendix C-A], we obtain the following surrogate sensing matrix  $\tilde{\mathbf{A}}$  and surrogate measurement vector  $\tilde{\mathbf{y}}$  given a Bernoulli( $q$ ) sensing matrix  $\mathbf{A}$  and its associated measurement vector  $\mathbf{y}$ :

$$\tilde{\mathbf{A}} = \frac{\mathbf{A}}{\sqrt{nq(1-q)}} - \frac{q\mathbf{1}_{n \times 1}\mathbf{1}_{p \times 1}^T}{\sqrt{nq(1-q)}}, \tilde{\mathbf{y}} = \frac{1}{(n-1)\sqrt{nq(1-q)}} \left( n\mathbf{y} - \sum_{l=1}^n y_l \mathbf{1}_{n \times 1} \right). \quad (11)$$

We use the surrogate matrix  $\tilde{\mathbf{A}}$  and surrogate measurement vector  $\tilde{\mathbf{y}}$  within the LASSO and WLASSO estimators, as will be shown in the next section. We note that  $\tilde{\mathbf{A}}$  and  $\tilde{\mathbf{y}}$  can be computed entirely from  $\mathbf{y}, \mathbf{A}, q$  without knowledge of the underlying signal. Moreover, we note that the REC holds with high probability for  $\tilde{\mathbf{A}}$ , as established in the lemma below which was proved in [2, Appendix C-B].

**Lemma 2.1.** *There exist positive constants  $c, c', c''$  such that with probability larger than  $1 - c' \exp(-c''n)$ ,  $\tilde{\mathbf{A}}$  satisfies  $REC(\kappa_1, \kappa_2)$  with parameters  $\kappa_1 := \frac{c}{q(1-q)} \sqrt{\frac{\ln p}{n}}, \kappa_2 := \frac{1}{4}$ .*

### 2.3.2. Data dependent weights

Given the surrogate sensing matrix  $\tilde{\mathbf{A}}$  and observations  $\tilde{\mathbf{y}}$ , we redefine the LASSO and WLASSO estimators via Equations (12) and (13) respectively, as given below:

$$\hat{\mathbf{x}}^L = \operatorname{argmin}_{\mathbf{x} \in \mathbb{R}^p} \|\tilde{\mathbf{y}} - \tilde{\mathbf{A}}\mathbf{x}\|_2^2 + \gamma \sum_{k=1}^p \beta |x_k|, \quad (12)$$

where  $\gamma > 2$  is a constant and  $\beta > 0$  is a data-dependent scalar.

$$\hat{\mathbf{x}}^{WL} = \operatorname{argmin}_{\mathbf{x} \in \mathbb{R}^p} \|\tilde{\mathbf{y}} - \tilde{\mathbf{A}}\mathbf{x}\|_2^2 + \gamma \sum_{k=1}^p \beta_k |x_k|, \quad (13)$$

where  $\gamma > 2$  is a constant and  $\beta_k > 0$  is the  $k$ th data-dependent scalar. The exact expressions of  $\beta$  and  $\beta_k$  depend on the observed data and form the crux of our work.

In this section, we now upper bound the term  $\left| \left( \tilde{\mathbf{A}}^T (\tilde{\mathbf{y}} - \tilde{\mathbf{A}} \mathbf{x}^*) \right)_k \right|$  and present data-dependent weights which satisfy Condition  $\mathcal{C}1$  with high-probability. We derive a single weight  $\beta$  for LASSO in Proposition 1, and then derive the weights  $\{\beta_k\}_{k=1}^p$  for the WLASSO in Proposition 2. The proofs of both propositions can be found in the Supplemental Material.

**Proposition 1. Weight for Lasso:**

Consider  $\mathbf{A}, \bar{\mathbf{R}} \in \mathbb{R}^{n \times p}$  and define  $W := \max_{i,j} (\bar{\mathbf{R}}^T \mathbf{A})_{ij}$  for  $1 \leq i \leq p, 1 \leq j \leq p$ ,  $\kappa := \sigma \ln(1 + q_a)$ , where  $\bar{\mathbf{R}}_{k,l} := \left( \frac{na_{l,k} - \sum_{l'=1}^n a_{l',k}}{n(n-1)q(1-q)} \right)^2$  for  $k = 1, \dots, p; l = 1, \dots, n$ . Consider the following assumptions:

A1.  $nq \geq 12 \max(q, 1 - q) \ln(p)$

A2.  $p \geq 2$

A3.  $\sigma < \frac{1}{\sqrt{2} \ln(1+q_a)} \left( \ln \left( \frac{1}{1 - (1 - \frac{1}{p^3})^{1/n}} \right) \right)^{-1/2}$

A4.  $\mathbf{A}$  is a Bernoulli Sensing Matrix.

If the aforementioned assumptions hold, then there exist positive constants  $c, c'$  such that with probability larger than  $1 - \frac{c'}{p}$ , the choice

$$\beta := \kappa \hat{\Lambda} \sqrt{6W \ln(p)} + c \left( \frac{3 \ln(p)}{n} + \frac{9 \max(q^2, (1 - q)^2)}{n^2 q (1 - q)} \ln(p)^2 \right) \hat{\Lambda}$$

satisfies Condition  $\mathcal{C}1$  (defined earlier in Equation (8)), where  $\hat{\Lambda}$  is an estimator of  $\|\mathbf{x}^*\|_1$  given by

$$\hat{\Lambda} := \frac{\sum_{i=1}^n y_i + \sqrt{\sum_{i=1}^n y_i^2} \frac{\kappa \sqrt{6 \ln(p)}}{1 - \kappa \sqrt{2g(3 \ln(p))}}}{nq - \sqrt{6nq(1 - q) \ln(p)} - \max(q, 1 - q) \ln(p)},$$

where for any  $\theta \in \mathbb{R}$ , we define  $g(\theta) := \ln \left( \frac{1}{1 - (1 - e^{-\theta})^{1/n}} \right)$ . Furthermore,  $c = 126$  works as long as  $n \geq 20$ .

**Proposition 2. Weights for WLasso**

With the same notations and assumptions as in Proposition 1, there exist positive constants  $c, c'$  such that with probability larger than  $1 - \frac{c'}{p}$ , the choice (depending on  $k$ )

$$\beta_k := \sqrt{\bar{\mathbf{R}}_k^T \mathbf{y}_2} \frac{\kappa \sqrt{6 \ln(p)}}{1 - \kappa \sqrt{2g(3 \ln(p))}} + c \left( \frac{3 \ln(p)}{n} + \frac{9 \max(q^2, (1-q)^2)}{n^2 q(1-q)} \ln(p)^2 \right) \hat{\Lambda}$$

satisfies Condition  $\mathcal{C}1$  (see Equation (8)), where  $\mathbf{y}_2 := \mathbf{y} \odot \mathbf{y}$ . Furthermore,  $c = 126$  works as long as  $n \geq 20$ .

**Comments on Proposition 1 and Proposition 2:**

1. We now argue that Assumption  $A\beta$  is reasonable for our RT-PCR noise model. Since  $n \geq 20$  and  $p > n$ , we have  $1 - \left(1 - \frac{1}{p^3}\right)^{\frac{1}{n}} > \frac{1}{np^3}$  by Bernoulli's inequality [30], [31, page 20]. Due to this, the expression  $\frac{1}{\sqrt{2 \ln(1+q_a)}} \ln^{-\frac{1}{2}}(np^3)$  acts as a lower bound on the RHS of the inequality in Assumption  $A\beta$  of Proposition 1. This lower bound decreases as  $n$  increases, as well as when  $q_a$  increases. Since we are operating in a compressive regime,  $n$  can be no greater than  $p$ . Moreover the largest possible value of  $q_a$  is 1. Hence the lower bound on the LHS is given by  $\frac{1}{2 \ln(2) \sqrt{2 \ln(p)}}$ . Therefore, if we consider  $\sigma < \frac{1}{2 \ln(2) \sqrt{2 \ln(p)}}$ , we always satisfy Assumption  $A\beta$  of Proposition 1. Given the small values of  $\sigma$  required in practice for the RT-PCR setting, as well as for the first-order expansion of the multiplicative noise model described in Equation (3), this restriction on  $\sigma$  is reasonable and holds true for a large range of  $p$ . For example, if  $p = 100$ , we have  $\sigma \leq 0.2377$ .
2. Under Assumption  $A1$  of Proposition 1, we avoid values of  $q$  very close to 0 or 1. Hence the weights  $\beta$  or  $\{\beta_k\}_{k=1}^p$  are not very large in value, as can be seen from Proposition 1 and Proposition 2. Thereby the upper bounds of the LASSO and WLASSO estimators are also not very large, as will be established in Proposition 3.
3. With Assumptions  $A1$  and  $A\beta$  in place, we can show that  $\hat{\Lambda}$ , that is the estimator for  $\|\mathbf{x}^*\|_1$ , is always positive. Note that Assumption  $A\beta$  can be re-written as  $\kappa \sqrt{2g(3 \ln p)} < 1$  by setting  $\theta = 3 \ln p$  and using the definition of  $\kappa$ . This makes the numerator of the expression for  $\hat{\Lambda}$

positive, whenever  $A\mathcal{B}$  is true as each element of  $y$  is non-negative. We now argue that the denominator is also positive, for which we denote  $m_q := \max(q, 1 - q)$  and set  $nq = hm_q \ln p$  for  $h \geq 12$  from Assumption A1. Then the denominator becomes  $\left((h - 1)m_q - \sqrt{6(1 - q)hm_q}\right) \ln p$  which is greater than or equal to  $\left((h - 1)m_q - m_q\sqrt{6h}\right) \ln p$  using the definition of  $m_q$ . For any  $h \geq 8$ , we see that this expression is always positive, since  $m_q$  and  $\ln p$  are both positive. At this point, we have established only lower bounds on  $\hat{\Lambda}$  and have not proved any upper bounds on its value in terms of  $\|\mathbf{x}^*\|_1$ . However, as will be shown in Sec. 3, the estimates are close to  $\|\mathbf{x}^*\|_1$  within a factor of two.

#### 2.4. Performance Bounds

In this section, we establish performance bounds for LASSO and WLASSO in the context of multiplicative lognormal Noise. For this, we present Proposition 3, which is derived directly from [2, Proposition 1] that accounts for the weighted  $l_1$  regularizer defined in Equation (13), combined with Propositions Proposition 1 and Proposition 2 derived here for our specific noise model.

#### Proposition 3. Performance Bounds for Lasso and WLasso

Fix  $\varepsilon > 0$  and consider the following:

$$\beta_{max} := \max_{k \in \{1, \dots, p\}} \beta_k, \beta_{min} := \min_{k \in \{1, \dots, p\}} \beta_k, \rho_\gamma := \gamma \frac{\gamma + 2}{\gamma - 2}$$

$$\mathbf{D} := \text{diag}(\beta_1, \dots, \beta_k, \dots, \beta_p),$$

where  $\gamma, \beta, \{\beta_k\}$  are parameters of the estimators presented in Section 2.2, and  $\mathbf{D}$  is a diagonal matrix with the  $k$ th diagonal element equal to  $\beta_k$ . For any vector  $\mathbf{z} \in \mathbb{R}^p$  and any set  $S \subseteq \{1, \dots, p\}$ , define vector  $\mathbf{z}_S$  such  $z_S(i) = z_i$  for all  $i \in S$  and  $z_S(i) = 0$  for all  $i \notin S$ .

Now consider that the following assumptions hold true:

B1.  $\gamma > 2$

B2.  $\{\beta_k\}_{k=1}^p$  and  $\beta$  satisfy the Condition  $\mathcal{C}1$  stated in Section 2.2

B3.  $\tilde{\mathbf{A}}$  satisfies the REC  $(\kappa_1, \kappa_2)$  property stated in Equation (9).

Then, there exists a universal constant  $c > 0$  such that for any set  $S \subseteq \{1, \dots, p\}$  for which

$$\|\boldsymbol{\beta}_S\|_2 \leq \beta_{\min} \frac{\kappa_2 - \varepsilon}{\kappa_1 \rho_\gamma},$$

the WLASSO estimator satisfies

$$\|\mathbf{x}^* - \hat{\mathbf{x}}^{\text{WL}}\|_2 \leq \frac{c\rho_\gamma}{\varepsilon^2} \|\boldsymbol{\beta}_S\|_2.$$

Furthermore, for any set  $S \subseteq \{1, \dots, p\}$  with  $s = |S|$  satisfying

$$\sqrt{s} \leq \frac{\kappa_2 - \varepsilon}{\kappa_1 \rho_\gamma}, \quad (14)$$

for  $\varepsilon > 0$ , the LASSO estimator satisfies

$$\|\mathbf{x}^* - \hat{\mathbf{x}}^{\text{L}}\|_2 \leq \frac{c\rho_\gamma}{\varepsilon^2} \beta \sqrt{s}. \quad (15)$$

### Comments on Proposition 3:

1. Performance bounds for LASSO in [15, Exercise 11.3, Eqn. 11.44a] or [2, Proposition 1] are derived for weakly sparse signals. In contrast, we operate in the purely sparse regime for  $\mathbf{x}^*$ , as weakly sparse signal models are not required for viral loads.
2. Consider the performance bounds for  $\hat{\mathbf{x}}^{\text{WL}}$  and  $\hat{\mathbf{x}}^{\text{L}}$  and the Assumption B2 from Proposition 3. Taking these into account, we observe that our motivation in Proposition 1 and Proposition 2 to find the smallest possible weights which satisfies the Condition C1 is well justified. Ideally we would want weights  $\beta_k$  such that  $\beta_k = |(\mathbf{A}^T(\mathbf{y} - \mathbf{A}\mathbf{x}^*))_k| \quad \forall k = 1, \dots, p$ . However, since the input signal  $\mathbf{x}^*$  is not observable, we can at best produce high probability approximations, as done in Proposition 1 and Proposition 2.
3. Upper bounds for both estimators increase with the  $s$ , the  $\ell_0$  norm of  $\mathbf{x}^*$ . As  $n$  increases, the upper bounds decrease, because the terms  $W$  in Proposition 1, and  $\sqrt{\bar{\mathbf{R}}_k^T \mathbf{y}_2}$  as well as  $\frac{3c \ln p}{n}$  in Proposition 2, all decrease with  $n$ . These trends with respect to  $s$  and  $n$  are quite intuitive.
4. As  $\|\mathbf{x}^*\|_1$  increases, we observe from Proposition 1 that all the  $y_i$  values will typically increase and hence  $\hat{\Lambda}$  will increase. Due to this,

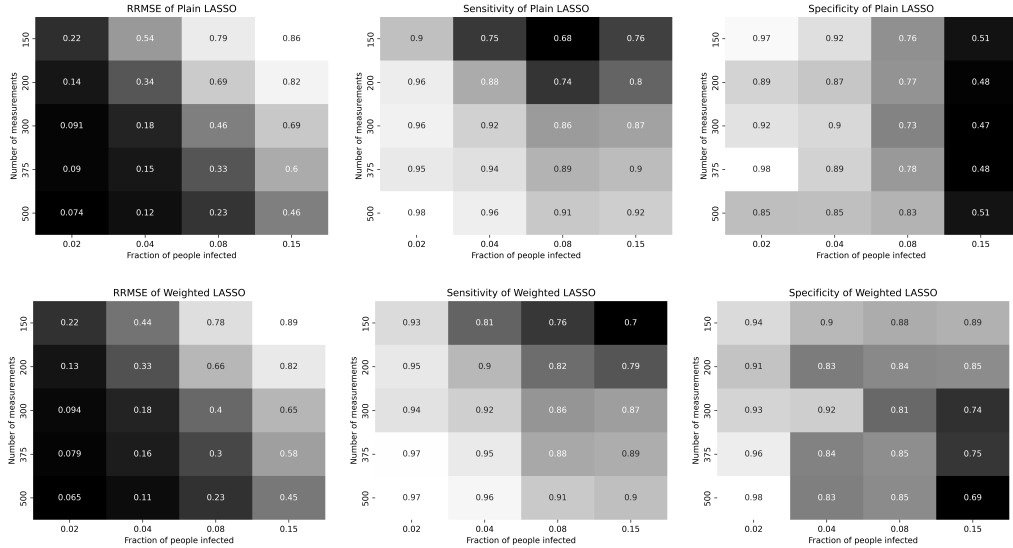


Figure 1: RRMSE, Sensitivity and Specificity values for  $q = 0.5$ , versus the number of measurements  $n$  and sparsity (fraction  $f_s$  of people infected). The top and bottom rows represent results for LASSO and WLASSO, respectively. Higher is better for Sensitivity and Specificity, and lower is better for RRMSE. Additional results with  $\sigma \in \{0.1, 0.15, 0.2\}$  can be found in Sec.4 of the Supplemental Material.

the upper bounds on  $\|\mathbf{x}^* - \hat{\mathbf{x}}^L\|_2$  and  $\|\mathbf{x}^* - \hat{\mathbf{x}}^{WL}\|_2$  for LASSO and WLASSO respectively will also increase. However, the *relative errors*  $\frac{\|\mathbf{x}^* - \hat{\mathbf{x}}^{WL}\|_2}{\|\mathbf{x}^*\|_1}$  and  $\frac{\|\mathbf{x}^* - \hat{\mathbf{x}}^L\|_2}{\|\mathbf{x}^*\|_1}$  remain constant. We emphasize the difference between this phenomenon and the trends observed in Poisson compressed sensing [20, 2, 17, 21], where the relative error actually *decreases* with  $\|\mathbf{x}^*\|_1$ . The reason for this difference is that the noise standard deviation is proportional to the *square root* of the signal value in case of Poisson noise, and proportional to the signal value in the multiplicative noise model of RT-PCR (see Equation (3)).

### 3. Numerical Results

We evaluate the derived expressions for the weights used in the LASSO and WLASSO estimators, using simulated signal reconstruction in pooled RT-PCR. In particular, we use the `cvxpy` [32, 33] Python package to solve the WLASSO problem using inputs  $\tilde{\mathbf{y}}, \mathbf{A}$ , which are derived from  $\mathbf{y}, \mathbf{A}$  as

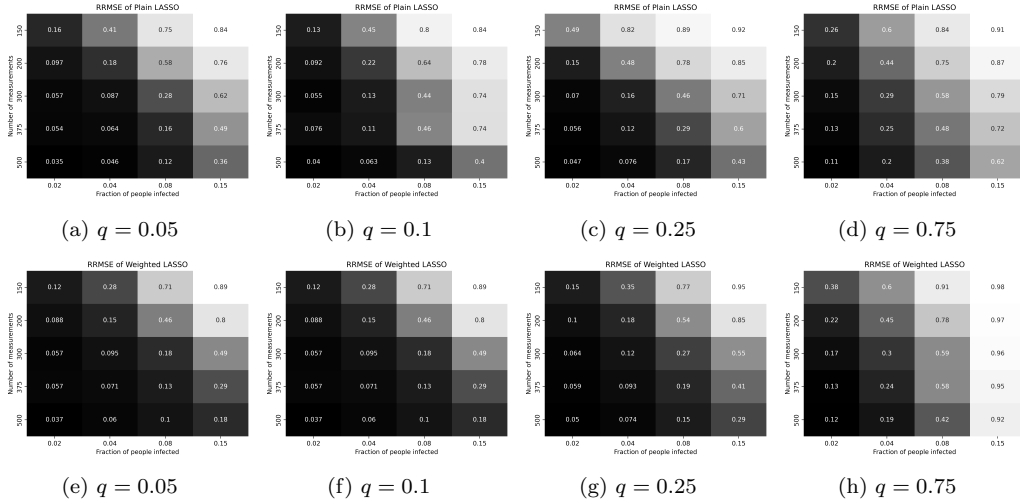


Figure 2: RRMSE values (lower is better) for  $q \in \{0.05, 0.1, 0.25, 0.75\}$  (left to right), versus the number of measurements  $n$  and  $f_s$  (fraction of people infected out of a total of  $p$ ). The top and bottom rows represent the results for LASSO and WLASSO, respectively.

explained in Sec. 2.3.1. In our simulations, we take the standard deviation of the (multiplicative) Gaussian noise  $\sigma$  to be 0.05, which is in tune with assumption A3 of Proposition 1 (see Comment 1 after Propositions 1 and 2). Additional results with  $\sigma \in \{0.1, 0.15, 0.2\}$  can be found in Sec.4 of the Supplemental Material. The amplification factor  $q_a$  is taken to be 0.95 (a reasonable choice since this factor is known to be close to 1 as the molecules roughly double in each RT-PCR cycle). Note that the values  $\sigma, q, q_a$  need not be specified as input to LASSO or WLASSO and are needed only for problem specification. The value of  $p$  (the number of samples being tested) is fixed at 1000 and the number of pools  $n$  is varied among  $\{150, 200, 300, 375, 500\}$ . The pooling matrix  $\mathbf{A}$  is a random Bernoulli matrix with each entry equal to 1 with probability  $q$ , and 0 otherwise, freshly sampled for each variation. We experiment with values of  $q$  in  $\{0.05, 0.1, 0.25, 0.5, 0.75\}$ . We mostly focus on the case of  $q = 0.5$  here - the complete set of plots will be made publicly available on GitHub along with the code used for simulation<sup>1</sup>. The underlying ground truth signal  $\mathbf{x}^*$  is chosen to have an  $\ell_0$  norm given by  $f_s \times p$  where the fraction  $f_s$  is sampled from  $\{0.02, 0.04, 0.08, 0.15\}$ . The significant non-

<sup>1</sup><https://github.com/sudoRicheek/Weighted-LASSO-MGN-Simulations>



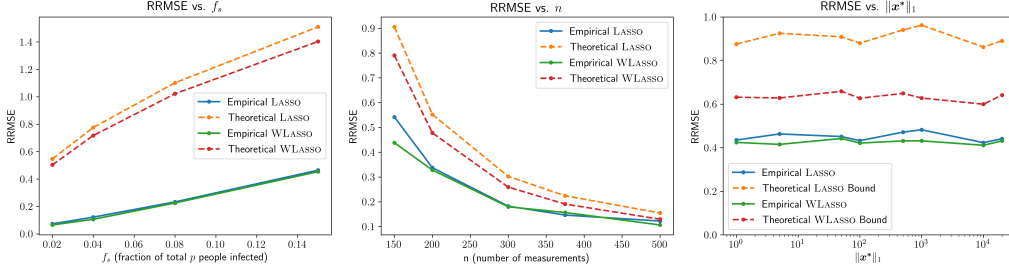


Figure 3: General trends of RRMSE vs  $\{f_s, n, \|\mathbf{x}^*\|_1\}$  (left to right). In each case, one of the parameters is varied, keeping the rest fixed to default values.

zero entries of  $\mathbf{x}^*$  are uniformly randomly sampled from the interval  $[1, 1000]$ , which reasonably represents the viral loads of infected individuals. The indices of the significant non-zero entries are drawn independently from a uniform distribution. The other entries are uniformly randomly sampled from  $[0, 0.2]$ . A viral load of 0.2 is used as a threshold to determine infected individuals from the reconstructed viral loads. However, slight variations in this threshold do not alter the Sensitivity and Specificity values stated in Figure 1.

For each combination of  $n, f_s, q$ , we execute 200 independent simulations and calculate averages of three intuitive and widely used measures: the RRMSE (Relative Root Mean-Squared-Error), the Sensitivity, and the Specificity, across the runs. The RRMSE is computed as  $\frac{\|\mathbf{x}^* - \hat{\mathbf{x}}\|_2}{\|\mathbf{x}^*\|_2}$ , where  $\hat{\mathbf{x}}$  represents the estimate of the ground truth vector  $\mathbf{x}$ . Let TP, TN, FP, FN denote the number of true positives, true negatives, false positives and false negatives respectively. The sensitivity is defined as  $\frac{TP}{TP + FN}$  (the probability of a positive test result for an unhealthy sample), whereas the specificity is defined as  $\frac{TN}{TN + FP}$  (the probability of a negative test result for a healthy sample). Higher values are better for sensitivity and specificity, whereas the opposite holds true for RRMSE. We report the measures as grid maps for both LASSO and WLASSO, with  $n$  and  $f_s$  being the independent variables selected from the ranges mentioned earlier. For each combination, we calculate a regularization factor  $\gamma$  to be multiplied to the weight  $\beta$  for LASSO or the weights  $\{\beta_k\}_{k=1}^p$  for WLASSO, using cross-validation on 5 preliminary runs.

We show the plots for the RRMSE values ( $q = 0.5$ ) in the first column of Figure 1. As expected, the RRMSE increases with the  $f_s$  (as a greater amount

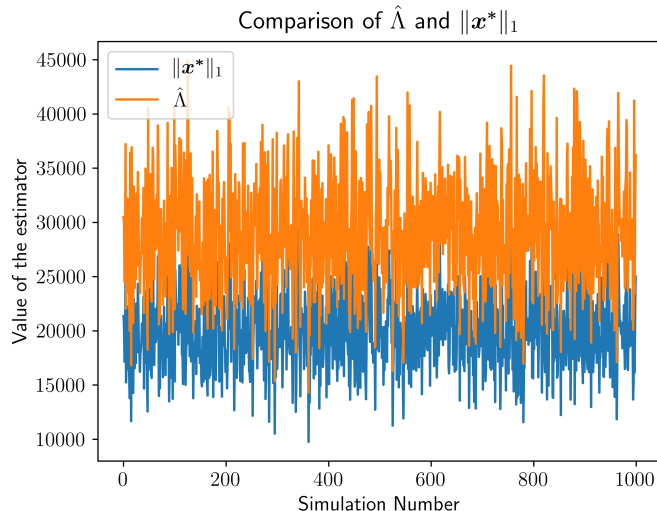


Figure 4: Comparison of the estimator  $\hat{\Lambda}$  with  $\|\mathbf{x}^*\|_1$  over a set of 1000 simulation runs (corresponding values of the two quantities are plotted together).

of information is now compressed down to the same dimensions) and decreases with the number of measurements (as more measurements capture more information). Out of LASSO and WLASSO, neither estimator is consistently superior to the other. This is, however unsurprising as the bounds we derive on the weights are worst-case bounds and may not apply to the average case. Nevertheless, the values obtained clearly demonstrate the suitability of the derived weights for reconstruction. We show the corresponding values for the Sensitivity and Specificity (for  $q = 0.5$ ) in the middle and rightmost columns of Figure 1 respectively. Interestingly, for higher fraction of people infected ( $f_s$ ), WLASSO achieves a better specificity while being competitive with LASSO in the sensitivity values. Both methods achieve high values on both measures at lower sparsity levels.

We also compare the obtained results with the cases when the value of  $q$  for the sensing matrix is chosen to be from  $\{0.05, 0.1, 0.25, 0.75\}$ . These results are shown in Figure 2. As can be seen, smaller values of  $q$  yield lower RRMSE values as the average number of participants per pool decreases with  $q$ . These trends will hold true as long as every sample participates in two or more pools and no pool is left empty.

As can be seen from Propositions 1, 2 and 3, the RRMSE value scale as  $O(\sqrt{s})$  w.r.t.  $s$ , as  $O(1/n)$  w.r.t.  $n$  and as  $O(1)$  w.r.t.  $\|\mathbf{x}^*\|_1$ , keeping all other

factors constant and set to their default values. We verified experimentally that these trends hold true, ignoring constant factors. The verification was performed over 500 independently generated signals. These trends are demonstrated in Figure 3.

Finally, the results in Propositions 1, 2 and 3 use an estimate of  $\|\mathbf{x}^*\|_1$ , denoted as  $\hat{\Lambda}$ . In Figure 4, we demonstrate that  $\hat{\Lambda}$  is a good estimate for  $\|\mathbf{x}^*\|_1$  and its value empirically never crosses  $2\|\mathbf{x}^*\|_1$ . This is shown for 1000 independent simulations. As an example, the average value of  $\|\mathbf{x}^*\|_1$  across 1000 simulations was  $\sim 19,900$  with a standard deviation of  $\sim 3500$ , whereas the average value of  $\hat{\Lambda}$  was  $\sim 28,900$  with a standard deviation of  $\sim 5200$ .

**Discussion:** In our group’s previous work [1], we have already shown comparisons between many different estimators for compressive RT-PCR. These estimators include LASSO, sparse Bayesian learning (SBL), orthogonal matching pursuit (OMP) among others. Out of these, LASSO is very simple to implement and performs empirically very well. However, there are no performance bounds for LASSO given this noise model (multiplicative log-normal) in RT-PCR in the literature. The aim of our paper is to fill that gap. Apart from this, there exists very little literature on compressive inversion given multiplicative noise in the measurements, [34] being a recent reference. However, the noise model in [34] is multiplicative *Gaussian* (which may be positive or negative), whereas the noise model in our paper is multiplicative *lognormal* (which is always non-negative). Hence, no comparison is possible in such a case. There certainly exist many algorithms for image filtering in multiplicative noise, however our work is on compressive inversion, and hence direct comparisons are not possible. Further note that first filtering  $\mathbf{y}$  and then reconstructing  $\mathbf{x}^*$  will not work well, as  $\mathbf{y}$  is not a sparse vector unlike  $\mathbf{x}^*$  which would lead to poor filtering performance.

#### 4. Conclusion

Despite extensive work on the theoretical guarantees for compressed sensing in the additive Gaussian Noise setting, current literature lacks performance bounds for the case of multiplicative lognormal Noise which describes the noise in the scenario of RT-PCR Group Testing. In this work we develop performance bounds for the weighted and unweighted LASSO problems in the case of multiplicative lognormal noise, and derive expressions for weights corresponding to these bounds. We then show via simulation that our weights yield good performance in practice. We hope that our efforts inspire future

work on more varied as well as general noise models in compressed sensing. A full analysis of performance bounds for the noise model without use of Taylor expansion, along the lines of [19], is an important avenue for future work. Our current work considers randomly generated Bernoulli matrices as pooling matrices. Extending our analysis to the important case of deterministic matrices [1] is another useful direction for future work. Multiplicative noise, albeit of a different form, also shows up in some other modalities such as synthetic aperture radar [35, 36, 34] and photo-acoustic tomography [37, Equation 17]. Developing compressed sensing bounds in such modalities is also another future research direction.

## References

- [1] S. Ghosh, R. Agarwal, M. A. Rehan, S. Pathak, P. Agarwal, Y. Gupta, S. Consul, N. Gupta, Ritika, R. Goenka, A. Rajwade, M. Gopalkrishnan, A compressed sensing approach to pooled RT-PCR testing for COVID-19 detection, *IEEE Open Journal of Signal Processing* 2 (2021) 248–264. doi:10.1109/ojosp.2021.3075913.
- [2] X. J. Hunt, P. Reynaud-Bouret, V. Rivoirard, L. Sansonnet, R. Willett, A data-dependent weighted LASSO under Poisson noise, *IEEE Transactions on Information Theory* 65 (3) (2018) 1589–1613. doi:10.1109/TIT.2018.2869578.
- [3] N. Jawerth, How is the COVID-19 virus detected using real time RT-PCR?, <https://www.iaea.org/newscenter/news/how-is-the-covid-19-virus-detected-using-real-time-rt-pcr>.
- [4] List of countries implementing pool testing strategy against COVID-19, [https://en.wikipedia.org/wiki/List\\_of\\_countries\\_implementing\\_pool\\_testing\\_strategy\\_against\\_COVID-19](https://en.wikipedia.org/wiki/List_of_countries_implementing_pool_testing_strategy_against_COVID-19), last retrieved, Oct 2021.
- [5] N. Shental, et al., Efficient high throughput SARS-CoV-2 testing to detect asymptomatic carriers, *Sci. Adv.* 6 (37) (Sep. 2020). doi:10.1126/sciadv.abc5961.
- [6] A. Heidarzadeh, K. Narayanan, Two-stage adaptive pooling with RT-qPCR for COVID-19 screening, in: ICASSP, 2021.

- [7] R. Goenka, S. Cao, C. Wong, A. Rajwade, D. Baron, Contact tracing information improves the performance of group testing algorithms (2021). URL <https://arxiv.org/abs/2106.02699>
- [8] R. Goenka, S.-J. Cao, C.-W. Wong, A. Rajwade, D. Baron, Contact tracing enhances the efficiency of covid-19 group testing, in: ICASSP 2021-2021 IEEE International Conference on Acoustics, Speech and Signal Processing (ICASSP), IEEE, 2021, pp. 8168–8172.
- [9] R. Dorfman, The Detection of Defective Members of Large Populations, *The Annals of Mathematical Statistics* 14 (4) (1943) 436 – 440. doi: 10.1214/aoms/1177731363.
- [10] Israelis introduce a method for accelerated covid-19 testing. URL <https://www.israel21c.org/israelis-introduce-method-for-accelerated-covid-19-testing/>
- [11] Corona pool testing increases worldwide capacities many times over. URL <https://healthcare-in-europe.com/en/news/corona-pool-testing-increases-worldwide-capacities-many-times-over.html>
- [12] D. B. Larremore, B. Wilder, E. Lester, S. Shehata, J. M. Burke, J. A. Hay, M. Tambe, M. Mina, R. Parker, Test sensitivity is secondary to frequency and turnaround time for COVID-19 screening, *Science Advances* 7 (1) (2021).
- [13] D. Donoho, Compressed sensing, *IEEE Transactions on Information Theory* 52 (4) (2006) 1289–1306. doi:10.1109/TIT.2006.871582.
- [14] M. Aldridge, O. Johnson, J. Scarlett, et al., Group testing: an information theory perspective, *Foundations and Trends® in Communications and Information Theory* 15 (3-4) (2019) 196–392.
- [15] T. Hastie, R. Tibshirani, M. Wainwright, *Statistical Learning with Sparsity: The LASSO and Generalizations*, CRC Press, 2015.
- [16] J. Huang, T. Zhang, The benefit of group sparsity, *The Annals of Statistics* 38 (4) (2010) 1978 – 2004.

- [17] Y. Li, G. Raskutti, Minimax optimal convex methods for Poisson inverse problems under  $\ell_q$ -ball sparsity, *IEEE Transactions on Information Theory* 64 (8) (2018) 5498–5512. doi:10.1109/TIT.2018.2850365.
- [18] S. Negahban, P. Ravikumar, M. J. Wainwright, B. Yu, A unified framework for high-dimensional analysis of M-estimators with decomposable regularizers, *Statistical Science* 27 (4) (2012) 538–557.
- [19] R. Chatterjee, Reconstruction of sparse signals under the influence of multiplicative log-normal noise using l1-regularization, <https://tinyurl.com/4w8rr5mz>, MSc Thesis, IIT Bombay (2021).
- [20] A. Rajwade, K. S. Gurumoorthy, Two penalized estimators based on variance stabilization transforms for sparse compressive recovery with Poisson measurement noise, *Signal Processing* 188 (2021) 108186.
- [21] P. Bohra, D. Garg, K. S. Gurumoorthy, A. Rajwade, Variance-stabilization-based compressive inversion under Poisson or Poisson–Gaussian noise with analytical bounds, *Inverse Problems* 35 (10) (2019) 105006.
- [22] V. Stojanovic, N. Nedic, D. Prsic, L. Dubonjic, Optimal experiment design for identification of arx models with constrained output in non-gaussian noise, *Applied Mathematical Modelling* 40 (13-14) (2016) 6676–6689.
- [23] V. Stojanovic, N. Nedic, Robust identification of oe model with constrained output using optimal input design, *Journal of the Franklin Institute* 353 (2) (2016) 576–593.
- [24] E. A. Daniel, et al., Pooled Testing Strategies for SARS-CoV-2 diagnosis: A comprehensive review, *Diagn Microbiol Infect Dis* 101 (2) (2021) 115432.
- [25] Y. Karlen, A. McNair, S. Perseguers, C. Mazza, N. Mermod, Statistical significance of quantitative PCR, *BMC bioinformatics* 8 (2007) 1–16.
- [26] T. Arildsen, T. Larsen, Compressed sensing with linear correlation between signal and measurement noise, *Signal Processing* 98 (2014) 275–283.

- [27] J. H. Pollard, A handbook of numerical and statistical techniques: with examples mainly from the life sciences, CUP Archive, 1979.
- [28] P. Gopal, S. Chandran, I. Svalbe, A. Rajwade, Low radiation tomographic reconstruction with and without template information, *Signal Processing* 175 (2020) 107582.
- [29] F.-X. Dupé, J. M. Fadili, J.-L. Starck, A proximal iteration for deconvolving Poisson noisy images using sparse representations, *IEEE Transactions on Image Processing* 18 (2) (2009) 310–321.
- [30] Bernoulli's inequality, [https://en.wikipedia.org/wiki/Bernoulli's\\_inequality](https://en.wikipedia.org/wiki/Bernoulli's_inequality).
- [31] D. A. Brannan, A first course in mathematical analysis, Cambridge University Press, 2006.
- [32] S. Diamond, S. Boyd, CVXPY: A Python-embedded modeling language for convex optimization, *Journal of Machine Learning Research* 17 (83) (2016) 1–5.
- [33] A. Agrawal, R. Verschueren, S. Diamond, S. Boyd, A rewriting system for convex optimization problems, *Journal of Control and Decision* 5 (1) (2018) 42–60.
- [34] W. Zhou, S. Jalali, A. Maleki, Compressed sensing in the presence of speckle noise, *IEEE Transactions on Information Theory* 68 (10) (2022) 6964–6980.
- [35] R. Pournaghshband, M. Modarres-Hashemi, A novel block compressive sensing algorithm for SAR image formation, *Signal Processing* 210 (2023) 109053.
- [36] G. Aubert, J.-F. Aujol, A variational approach to removing multiplicative noise, *SIAM journal on applied mathematics* 68 (4) (2008) 925–946.
- [37] S. Arridge, P. Beard, M. Betcke, B. Cox, N. Huynh, F. Lucka, O. Ogunlade, E. Zhang, Accelerated high-resolution photoacoustic tomography via compressed sensing, *Physics in Medicine & Biology* 61 (24) (2016) 8908.

# Supplemental Material for ‘Performance Bounds for LASSO under Multiplicative LogNormal Noise: Applications to Pooled RT-PCR Testing’

Richeek Das<sup>a</sup>, Aaron Jerry Ninan<sup>b</sup>, Adithya Bhaskar<sup>a</sup>, Ajit Rajwade<sup>a</sup>

<sup>a</sup>*Indian Institute of Technology Bombay, Department of Computer Science and Engineering,*

<sup>b</sup>*Indian Institute of Technology Bombay, Department of Electrical Engineering,*

---



---

This supplemental material contains a brief introduction in Section 1, statements of key propositions in Section 2 and their proofs in Section 3, and some additional experimental results in Section 4.

## 1. Preliminaries

We reproduce expressions for the noise model from the main paper here below. In all of the following,  $\mathbf{x}^* \in \mathbb{R}^p$  is the ground truth vector of viral loads,  $\mathbf{y} \in \mathbb{R}^n$  is the measurement vector,  $\mathbf{w} \in \mathbb{R}^m$  is the noise vector, and  $\mathbf{A} \in \{0, 1\}^{n \times p}$  is the pooling matrix, with entries drawn independently from Bernoulli( $q$ ) where  $q \in (0, 1)$ . We also have  $n < p$ .

$$y_j = \mathbf{A}^j \mathbf{x}^* (1 + q_a)^{w_j}, \quad (1)$$

where  $q_a \in (0, 1]$  is an amplification factor and  $w_j \sim \mathcal{N}(0, \sigma^2)$  where  $\sigma < 1$ . Using a first order Taylor series expansion, we have:

$$y_j \approx \mathbf{A}^j \mathbf{x}^* + [\mathbf{A}^j \mathbf{x}^* \ln(1 + q_a)] w_j. \quad (2)$$

As argued in the main paper, this approximation is good because  $\sigma < 1$  and due to division by factors larger than 1 or multiplication by factors less than 1

---

*Email addresses:* [richeek@cse.iitb.ac.in](mailto:richeek@cse.iitb.ac.in) (Richeek Das),  
[aaronjerry12@gmail.com](mailto:aaronjerry12@gmail.com) (Aaron Jerry Ninan), [adithyabhaskar@cse.iitb.ac.in](mailto:adithyabhaskar@cse.iitb.ac.in)  
 (Adithya Bhaskar), [ajitvr@cse.iitb.ac.in](mailto:ajitvr@cse.iitb.ac.in) (Ajit Rajwade)



in higher order terms. We also reproduce expressions for the surrogate sensing matrix  $\tilde{\mathbf{A}}$  (for a Bernoulli ( $q$ ) sensing matrix  $\mathbf{A}$ ) and surrogate measurement vector  $\tilde{\mathbf{y}}$  from the main paper here below:

$$\tilde{\mathbf{A}} = \frac{\mathbf{A}}{\sqrt{nq(1-q)}} - \frac{q\mathbf{1}_{n \times 1}\mathbf{1}_{p \times 1}^T}{\sqrt{nq(1-q)}}. \quad (3)$$

$$\tilde{\mathbf{y}} = \frac{1}{(n-1)\sqrt{nq(1-q)}} \left( n\mathbf{y} - \sum_{l=1}^n y_l \mathbf{1}_{n \times 1} \right). \quad (4)$$

Given the surrogate sensing matrix  $\tilde{\mathbf{A}}$  and observations  $\tilde{\mathbf{y}}$ , we redefine the LASSO and WLASSO estimators via Equations (5) and (6) respectively, as given below:

$$\hat{\mathbf{x}}^L = \underset{\mathbf{x} \in \mathbb{R}^p}{\operatorname{argmin}} \|\tilde{\mathbf{y}} - \tilde{\mathbf{A}}\mathbf{x}\|_2^2 + \gamma \sum_{k=1}^p \beta |x_k|, \quad (5)$$

where  $\gamma > 2$  is a constant and  $\beta > 0$  is a data-dependent scalar.

$$\hat{\mathbf{x}}^{WL} = \underset{\mathbf{x} \in \mathbb{R}^p}{\operatorname{argmin}} \|\tilde{\mathbf{y}} - \tilde{\mathbf{A}}\mathbf{x}\|_2^2 + \gamma \sum_{k=1}^p \beta_k |x_k|, \quad (6)$$

where  $\gamma > 2$  is a constant and  $\beta_k > 0$  is the  $k$ th data-dependent scalar. The exact expressions of  $\beta$  and  $\beta_k$  depend on the observed data and form the crux of our work.

We want the *smallest* possible values of  $\beta_k$  which would faithfully satisfy the Condition  $\mathcal{C}1$  (defined below) with high probability. This serves as our primary objective in deriving the data-dependent weights for our noise model

$$\text{Condition } \mathcal{C}1 \text{ on } (\{\beta_k\}_k) : |(\mathbf{A}^T(\mathbf{y} - \mathbf{A}\mathbf{x}^*))_k| \leq \beta_k \quad \forall k = 1, \dots, p. \quad (7)$$

## 2. Statements of the Propositions

### Proposition 1. Weight for Lasso:

Consider  $\mathbf{A}, \bar{\mathbf{R}} \in \mathbb{R}^{n \times p}$  and define the following:

$$W := \max_{i,j} (\bar{\mathbf{R}}^T \mathbf{A})_{ij} \quad \text{for } 1 \leq i \leq p, 1 \leq j \leq p, \quad \text{and} \quad \kappa := \sigma \ln(1 + q_a)$$

where  $\bar{R}_{k,l} = \left( \frac{na_{l,k} - \sum_{l'=1}^n a_{l',k}}{n(n-1)q(1-q)} \right)^2$  for  $k = 1, \dots, p; l = 1, \dots, n$ .

Consider the following assumptions:

A1.  $nq \geq 12 \max(q, 1 - q) \ln(p)$

A2.  $p \geq 2$

A3.  $\sigma < \frac{1}{\sqrt{2} \ln(1+q_a)} \left( \ln \left( \frac{1}{1 - \left(1 - \frac{1}{p^3}\right)^{1/n}} \right) \right)^{-1/2}$

A4.  $\mathbf{A}$  is a Bernoulli Sensing Matrix.

If the aforementioned assumptions hold, then there exist positive constants  $c, c'$  such that with probability larger than  $1 - \frac{c'}{p}$ , the choice

$$\beta := \kappa \hat{\Lambda} \sqrt{6W \ln(p)} + c \left( \frac{3 \ln(p)}{n} + \frac{9 \max(q^2, (1 - q)^2)}{n^2 q (1 - q)} \ln(p)^2 \right) \hat{\Lambda}$$

satisfies Condition  $\mathcal{C}1$  (defined earlier in Equation (7)), where  $\hat{\Lambda}$  is an estimator of  $\|\mathbf{x}^*\|_1$  given by

$$\hat{\Lambda} := \frac{\sum_{i=1}^n y_i + \sqrt{\sum_{i=1}^n y_i^2} \frac{\kappa \sqrt{6 \ln(p)}}{1 - \kappa \sqrt{2g(3 \ln(p))}}}{nq - \sqrt{6nq(1 - q) \ln(p)} - \max(q, 1 - q) \ln(p)},$$

where for any  $\theta \in \mathbb{R}$ , we define

$$g(\theta) := \ln \left( \frac{1}{1 - (1 - e^{-\theta})^{1/n}} \right).$$

Furthermore,  $c = 126$  works as long as  $n \geq 20$ .

### Proposition 2. Weights for WLasso

With the same notations and assumptions as in Proposition 1, there exist positive constants  $c, c'$  such that with probability larger than  $1 - \frac{c'}{p}$ , the choice (depending on  $k$ )

$$\beta_k := \sqrt{\frac{\bar{\mathbf{R}}_k^T \mathbf{y}_2}{1 - \kappa \sqrt{2g(3 \ln(p))}}} \frac{\kappa \sqrt{6 \ln(p)}}{1 - \kappa \sqrt{2g(3 \ln(p))}} + c \left( \frac{3 \ln(p)}{n} + \frac{9 \max(q^2, (1 - q)^2)}{n^2 q (1 - q)} \ln(p)^2 \right) \hat{\Lambda}$$

satisfies Condition  $\mathcal{C}1$  (see Equation (7)), where  $\mathbf{y}_2 := \mathbf{y} \odot \mathbf{y}$ . Furthermore,  $c = 126$  works as long as  $n \geq 20$ .

### 3. Proof of Proposition 1 and Proposition 2

To choose data-dependent weights, we need to satisfy the Condition  $\mathcal{C}1$ . From Equation (7), we know that if each  $\beta_k$  in the WLASSO is close to  $\left| \left( \tilde{\mathbf{A}}^T (\tilde{\mathbf{y}} - \tilde{\mathbf{A}}\mathbf{x}^*) \right)_k \right|$  then the risk bounds on both LASSO and WLASSO approach the oracle least squares estimator [1], [2, Sec. I-B]. Hence, our target is to find the smallest possible  $\beta_k$ 's that satisfy the Condition  $\mathcal{C}1$  in Equation (7). To do this, we derive high-probability concentration inequalities to upper bound the LHS of Equation (7). The rest of the proof here explains how we proceed with this.

For all vectors  $\mathbf{r} \in \mathbb{R}^n$ , we can deduce the following starting from Equation (2) as follows:

$$\begin{aligned} \sum_j r_j y_j &= \sum_j r_j \mathbf{A}^j \mathbf{x}^* + \sum_j r_j \mathbf{A}^j \mathbf{x}^* \ln(1 + q_a) w_j \\ &\implies \mathbf{r}^T \mathbf{y} \sim \mathcal{N} \left[ \mathbf{r}^T \mathbf{A} \mathbf{x}^*, \mathbf{r}_2^T (\mathbf{A} \mathbf{x}^*)_{2\kappa^2} \right], \end{aligned} \quad (8)$$

where  $\kappa := \sigma \ln(1 + q_a)$  and  $\mathbf{r}_2 := \mathbf{r} \odot \mathbf{r}$ , that is the element-wise square of each element in the vector  $\mathbf{r}$ . The implication above follows because of the mutual independence of  $\{w_j\}_{j=1}^n$ .

Now let us rewrite  $\left( \tilde{\mathbf{A}}^T (\tilde{\mathbf{y}} - \tilde{\mathbf{A}}\mathbf{x}^*) \right)$  as:

$$\tilde{\mathbf{A}}^T (\tilde{\mathbf{y}} - \tilde{\mathbf{A}}\mathbf{x}^*) = \mathbf{t}_1 + \mathbf{t}_2 \quad (9)$$

$$= \underbrace{\frac{1}{nq(1-q)} \left( \frac{n}{n-1} \mathbf{A}^T - \frac{\mathbf{A}^T \mathbf{1}_{n \times 1} \mathbf{1}_{n \times 1}^T}{n-1} \right)}_{\mathbf{t}_1} (\mathbf{y} - \mathbf{A} \mathbf{x}^*) + \quad (10)$$

$$\underbrace{\frac{1}{nq(1-q)} \left( \frac{\mathbf{A}^T \mathbf{A} \mathbf{x}^* - \mathbf{A}^T \mathbf{1}_{n \times 1} \mathbf{1}_{n \times 1}^T \mathbf{A} \mathbf{x}^*}{n-1} + q \|\mathbf{x}^*\|_1 \mathbf{A}^T \mathbf{1}_{n \times 1} + q \mathbf{1}_{p \times 1} \mathbf{1}_{n \times 1}^T \mathbf{A} \mathbf{x}^* - q^2 n \|\mathbf{x}^*\|_1 \mathbf{1}_{p \times 1} \right)}_{\mathbf{t}_2} \quad (11)$$

which is easy to observe since  $\sum_{l=1}^n \mathbf{y}_l \mathbf{1}_{n \times 1} = \mathbf{1}_{n \times 1} \mathbf{1}_{1 \times n} \mathbf{y}$  and  $\mathbf{1}_{1 \times n} \mathbf{1}_{1 \times n}^T = n$ . Then we have:

$$\left( \tilde{\mathbf{A}}^T (\tilde{\mathbf{y}} - \tilde{\mathbf{A}}\mathbf{x}^*) \right)_k = \mathbf{R}_k^T (\mathbf{y} - \mathbf{A} \mathbf{x}^*) + b_k(\mathbf{A}, \mathbf{x}^*) \quad (12)$$

where  $b_k(\mathbf{A}, \mathbf{x}^*)$  is defined below, and  $\mathbf{R}_k \in \mathbb{R}^n$  is the  $k$ -th column of the matrix  $\mathbf{R} \in \mathbb{R}^{n \times p}$  as defined below:

$$\mathbf{R}^T := \frac{1}{nq(1-q)} \left( \frac{n}{n-1} \mathbf{A}^T - \frac{\mathbf{A}^T \mathbf{1}_{n \times 1} \mathbf{1}_{n \times 1}^T}{n-1} \right), \quad (13)$$

$$b_k(\mathbf{A}, \mathbf{x}^*) := t_{2,k}; t_{1k} = \mathbf{R}_k^T (\mathbf{y} - \mathbf{A} \mathbf{x}^*). \quad (14)$$

Our aim is to upper bound  $\|\tilde{\mathbf{A}}^T(\tilde{\mathbf{y}} - \tilde{\mathbf{A}}\mathbf{x}^*)\|_\infty$ , for which we need to upper bound  $\|\mathbf{t}_1\|_\infty + \|\mathbf{t}_2\|_\infty$  in order to derive the constant weight in Proposition 1. To derive the non-constant weights in Proposition 2 we set bounds on  $|t_{1,k}| + |t_{2,k}|$ . In the initial stages, we will see that all these bounds will depend on the input signal  $\mathbf{x}^*$  or some quantities derived from it. Later on, we will present bounds and machinery to replace terms directly involving  $\mathbf{x}^*$  with computable quantities.

Since we are using Bernoulli sensing matrices, we can reuse the calculations presented in [2, Appendix C]. From [2, Appendix C], we state the probabilistic upper bound on  $\|\mathbf{t}_2\|_\infty$  with some assumptions in the following Lemma 1:

**Lemma 1.** *Consider positive constants  $c_1$  and  $c_2$ . Given  $n \geq 2$  and  $\theta > 1$ , with probability larger than  $1 - c_1 p^2 e^{-\theta}$ , we have:*

$$\|\mathbf{t}_2\|_\infty \leq c_2 \left( \frac{\theta}{n} + \frac{\max(q^2, (1-q)^2)}{n^2 q(1-q)} \theta^2 \right) \|\mathbf{x}^*\|_1, \quad (15)$$

where  $c_2 = 126$  works when  $n \geq 20$ .

The bound on  $\|\mathbf{t}_2\|_\infty$  in Lemma 1, requires the knowledge of  $\|\mathbf{x}^*\|_1$ . Since it is generally impossible to have knowledge of the  $l_1$  norm of the input signal in a reconstruction problem, we derive an estimator for it later in the proof. At first, we develop the required intermediate bounds and estimators needed to set concentration bounds on  $|t_{1,k}|$ . From Equation (9) we observe:

$$t_{1,k} = \mathbf{R}_k^T (\mathbf{y} - \mathbf{A} \mathbf{x}^*), \quad (16)$$

where  $\mathbf{R}$  is as defined in Equation 13 and  $\mathbf{R}_k$  is its  $k$ th column. That is, for all  $l = 1, \dots, n$ , and  $k = 1, \dots, p$  we have:

$$R_{k,l} = \frac{n a_{l,k} - \sum_{l'=1}^n a_{l',k}}{n(n-1)q(1-q)}. \quad (17)$$

To bound  $\|\mathbf{t}_1\|_\infty$  and  $|t_{1,k}|$ , we will need some concentration inequalities on  $\|\mathbf{R}^T(\mathbf{y} - \mathbf{A} \mathbf{x}^*)\|_\infty$ . With this goal in mind, we now develop the required concentration inequalities for our case of multiplicative lognormal noise.

### 3.1. Concentration Bounds for Multiplicative Lognormal Noise

With the same terminology presented in Section 3, we follow the lines of the proof of Bernstein's inequality. Let  $z := \mathbf{r}^T \mathbf{y}$  and  $\tilde{z} := \mathbf{r}^T \mathbf{A} \mathbf{x}^*$ , where  $\mathbf{r} \in \mathbb{R}^n$ . Therefore for all  $\lambda \in \mathbb{R} : \lambda > 0$  we have:

$$\mathbb{E} \left( e^{\lambda(z-\tilde{z})} | \mathbf{A} \right) = \mathbb{E} \left( e^{\lambda \mathbf{r}^T [\mathbf{y} - \mathbf{A} \mathbf{x}^*]} | \mathbf{A} \right) = \mathbb{E} \left( e^{\lambda \mathbf{r}^T \mathbf{y}} | \mathbf{A} \right) e^{-\lambda \mathbf{r}^T \mathbf{A} \mathbf{x}^*}.$$

Using the standard expression for the moment generating function (MGF) of  $\mathbf{r}^T \mathbf{y}$ , which is Gaussian distributed as per Section 3, we have:

$$\begin{aligned} \mathbb{E} \left( e^{\lambda(z-\tilde{z})} | \mathbf{A} \right) &= \exp \left( \mathbf{r}^T \mathbf{A} \mathbf{x}^* \lambda + \frac{1}{2} \mathbf{r}_2^T (\mathbf{A} \mathbf{x}^*)_2 \kappa^2 \lambda^2 \right) \exp \left( -\lambda \mathbf{r}^T \mathbf{A} \mathbf{x}^* \right) \\ &= \exp \left( \frac{1}{2} \mathbf{r}_2^T (\mathbf{A} \mathbf{x}^*)_2 \kappa^2 \lambda^2 \right), \end{aligned}$$

where  $\mathbf{r}_2 := \mathbf{r} \odot \mathbf{r}$  as defined before and  $\lambda$  is the MGF parameter. Therefore,

$$\mathbb{E} \left( e^{\lambda(z-\tilde{z})} | \mathbf{A} \right) = \exp \left( \frac{\kappa^2 \lambda^2 v}{2} \right), \text{ where } v := \mathbf{r}_2^T (\mathbf{A} \mathbf{x}^*)_2. \quad (18)$$

Using Markov's Inequality, for all  $u \in \mathbb{R} : u > 0$

$$\mathbb{P}(z - \tilde{z} \geq u) \leq \exp \left( \frac{\kappa^2 \lambda^2 v}{2} - \lambda u \right). \quad (19)$$

We need to find the minimal upper bound, so we optimize on  $\lambda$ , thus yielding  $\lambda = \frac{u}{\kappa^2 v}$ . This gives us

$$\mathbb{P}(z - \tilde{z} \geq u) \leq \exp \left( -\frac{u^2}{2\kappa^2 v} \right). \quad (20)$$

Denoting the upper bound on the probability by  $e^{-\theta}$ , we obtain  $u = \kappa \sqrt{2\theta v}$ . Therefore we have our first bound

$$\mathbb{P} \left( \mathbf{r}^T \mathbf{y} - \mathbf{r}^T \mathbf{A} \mathbf{x}^* \geq \kappa \sqrt{2\theta v} \right) \leq e^{-\theta}. \quad (21)$$

Replacing  $\mathbf{r}$  by  $-\mathbf{r}$  and using the symmetry of a Gaussian distribution, we obtain the following via a union bound:

$$\mathbb{P} \left( |\mathbf{r}^T \mathbf{y} - \mathbf{r}^T \mathbf{A} \mathbf{x}^*| \geq \kappa \sqrt{2\theta v} \right) \leq 2e^{-\theta}. \quad (22)$$

To proceed with the proof, we need to find bounds for  $|\mathbf{R}_l^T (\mathbf{y} - \mathbf{A} \mathbf{x}^*)|$  such that they are independent of the input signal  $\mathbf{x}^*$ . In our case, the above bounds in Equation (21) and Equation (22) still depend on  $v := \mathbf{r}_2^T (\mathbf{A} \mathbf{x}^*)_2$ . We still need to find bounds for  $v$ .

### 3.2. Bounding $v = \mathbf{r}_2^T(\mathbf{A}\mathbf{x}^*)_2$

From Equation (2), we obtain the following result when we set  $\eta_i := w_i/\sigma$  where  $w_i \sim \mathcal{N}(0, \sigma^2)$ :

$$(\mathbf{A}\mathbf{x}^*)_i^2 = \frac{\mathbf{y}_i^2}{(1 + \eta_i\kappa)^2}. \quad (23)$$

By definition of  $\eta_i$ , we have  $\eta_i \sim \mathcal{N}(0, 1)$ . Hence, we can use a standard Chernoff bound to obtain an upper concentration bound on  $\eta_i$  with any  $\varphi \in \mathbb{R}$ :

$$\mathbb{P}\left(\eta_i \leq -\frac{\varphi}{\kappa}\right) \leq \exp\left(-\frac{\varphi^2}{2\kappa^2}\right). \quad (24)$$

Therefore under the assumption  $\varphi < 1$ , with probability  $\geq 1 - \exp\left(-\frac{\varphi^2}{2\kappa^2}\right)$ , we have

$$\frac{\mathbf{y}_i^2}{(1 + \eta_i\kappa)^2} < \frac{\mathbf{y}_i^2}{(1 - \varphi^2)}. \quad (25)$$

Hence, we have:

$$\mathbb{P}\left(\mathbf{r}_i^2(\mathbf{A}\mathbf{x}^*)_i^2 \geq \frac{\mathbf{r}_i^2\mathbf{y}_i^2}{(1 - \varphi)^2}\right) \leq \exp\left(-\frac{\varphi^2}{2\kappa^2}\right) \quad (26)$$

$$\implies \mathbb{P}\left(\mathbf{r}_i^2(\mathbf{A}\mathbf{x}^*)_i^2 < \frac{\mathbf{r}_i^2\mathbf{y}_i^2}{(1 - \varphi)^2}\right) > 1 - \exp\left(-\frac{\varphi^2}{2\kappa^2}\right) \quad (27)$$

The event  $\mathbf{r}_2^T(\mathbf{A}\mathbf{x}^*)_2 < \frac{\mathbf{r}_2^T\mathbf{y}_2}{(1 - \varphi)^2}$  will hold true when each of the events  $\mathcal{E}_i := \mathbf{r}_i^2(\mathbf{A}\mathbf{x}^*)_i^2 < \frac{\mathbf{r}_i^2\mathbf{y}_i^2}{(1 - \varphi)^2}$  (across  $i$ ) occurs. Given the mutual independence of  $w_i$ 's, we know that the events  $\{\mathcal{E}_i\}_{i=1}^n$  are independent. Hence, we obtain:

$$\mathbb{P}\left(\mathbf{r}_2^T(\mathbf{A}\mathbf{x}^*)_2 < \frac{\mathbf{r}_2^T\mathbf{y}_2}{(1 - \varphi)^2}\right) > \left(1 - \exp\left(-\frac{\varphi^2}{2\kappa^2}\right)\right)^n. \quad (28)$$

$$\implies \mathbb{P}\left(\mathbf{r}_2^T(\mathbf{A}\mathbf{x}^*)_2 \geq \frac{\mathbf{r}_2^T\mathbf{y}_2}{(1 - \varphi)^2}\right) \leq 1 - \left(1 - \exp\left(-\frac{\varphi^2}{2\kappa^2}\right)\right)^n. \quad (29)$$

Setting  $\exp(-\theta) = 1 - \left(1 - \exp\left(-\frac{\varphi^2}{2\kappa^2}\right)\right)^n$ , we obtain:

$$\varphi = \kappa \sqrt{2 \ln \left( \frac{1}{1 - (1 - e^{-\theta})^{1/n}} \right)}.$$

Since  $\varphi < 1$ , the earlier equation can be restated more concisely in the form of a new function  $g(\theta)$ :

$$g(\theta) = \ln \left( \frac{1}{1 - (1 - e^{-\theta})^{1/n}} \right) \quad \text{and} \quad \kappa \sqrt{2g(\theta)} < 1. \quad (30)$$

**Note:** Expanding Equation (30) leads to our Assumption  $A\beta$  in Proposition 1 and Proposition 2.

Under the above assumption, we have our high-probability upper bound on  $v = \mathbf{r}_2^T(\mathbf{A}\mathbf{x}^*)_2$  as:

$$\mathbb{P} \left( \mathbf{r}_2^T(\mathbf{A}\mathbf{x}^*)_2 \geq \frac{\mathbf{r}_2^T \mathbf{y}_2}{(1 - \kappa \sqrt{2g(\theta)})^2} \right) \leq e^{-\theta} \quad (31)$$

Combining Equation (21), Equation (22) and Equation (31) we obtain the required concentration inequalities on  $|\mathbf{R}_i^T(\mathbf{y} - \mathbf{A}\mathbf{x}^*)|$ . For instance, Equation (21) and Equation (31) can be easily combined through a union bound on the following two events:

$$\mathcal{X}_1 := \mathbf{r}^T \mathbf{y} - \mathbf{r}^T \mathbf{A}\mathbf{x}^* \geq \kappa \sqrt{2\theta \mathbf{r}_2^T(\mathbf{A}\mathbf{x}^*)_2} \quad (32)$$

$$\mathcal{X}_2 := \mathbf{r}_2^T(\mathbf{A}\mathbf{x}^*)_2 \geq \frac{\mathbf{r}_2^T \mathbf{y}_2}{(1 - \kappa \sqrt{2g(\theta)})^2}, \quad (33)$$

since our target event  $\mathcal{X}_3 := \left( \mathbf{r}^T \mathbf{y} - \mathbf{r}^T \mathbf{A}\mathbf{x}^* \geq \sqrt{\mathbf{r}_2^T \mathbf{y}_2} \frac{\kappa \sqrt{2\theta}}{1 - \kappa \sqrt{2g(\theta)}} \right)$  might hold true even if one of events  $\mathcal{X}_1$  or  $\mathcal{X}_2$  does not occur. We state this formally in the following Lemma 2.

**Lemma 2.** *Let  $\mathbf{R} \in \mathbb{R}^{n \times p}$  be any real-valued matrix and  $\bar{\mathbf{R}} = \mathbf{R} \odot \mathbf{R}$  be a matrix containing the element-wise squares of  $\mathbf{R}$ , then the following high-probability upper bounds hold*

$$\mathbb{P} \left( \mathbf{R}_i^T(\mathbf{y} - \mathbf{A}\mathbf{x}^*) \geq \sqrt{\bar{\mathbf{R}}_i^T \mathbf{y}_2} \frac{\kappa \sqrt{2\theta}}{1 - \kappa \sqrt{2g(\theta)}} \right) \leq 2e^{-\theta} \quad (34)$$

$$\mathbb{P} \left( |\mathbf{R}_i^T(\mathbf{y} - \mathbf{A}\mathbf{x}^*)| \geq \sqrt{\bar{\mathbf{R}}_i^T \mathbf{y}_2} \frac{\kappa \sqrt{2\theta}}{1 - \kappa \sqrt{2g(\theta)}} \right) \leq 3e^{-\theta} \quad (35)$$

under the assumption  $\kappa\sqrt{2g(\theta)} < 1$  where,

$$g(\theta) = \ln\left(\frac{1}{1 - (1 - e^{-\theta})^{1/n}}\right) \quad \text{and} \quad \kappa := \ln(1 + q_a)\sigma$$

### 3.3. Bounding $|t_{1,k}|$ and $\|\mathbf{t}_1\|_\infty$

With Lemma 2 in place, we can set the required bounds on  $|t_{1,k}|$  and  $\|\mathbf{t}_1\|_\infty$  for the non-constant (weighted) and constant (plain) weights respectively. From Equation (16) we know:

$$t_{1,k} = \mathbf{R}_k^T(\mathbf{y} - \mathbf{A}\mathbf{x}^*) \quad \text{and} \quad R_{k,l} = \frac{na_{l,k} - \sum_{l'=1}^n a_{l',k}}{n(n-1)q(1-q)}$$

**Note:**  $\mathbf{R} \in \mathbb{R}^{n \times p}$  and  $\mathbf{R}_k \in \mathbb{R}^n$ ,  $k = 1, \dots, p$  and  $l = 1, \dots, n$ .

Define,  $\bar{R}_{k,l} = R_{k,l}^2$ , i.e.  $\bar{\mathbf{R}} = \mathbf{R} \odot \mathbf{R}$ . By Equation (35) of Lemma 2, we can directly obtain a bound for  $|t_{1,k}|$ . We have the following result with probability  $\geq 1 - 3e^{-\theta}$ :

$$|t_{1,k}| \leq \sqrt{\bar{\mathbf{R}}_k^T \mathbf{y}_2} \frac{\kappa\sqrt{2\theta}}{1 - \kappa\sqrt{2g(\theta)}}. \quad (36)$$

For constant weights we need to find  $\|\mathbf{t}_1\|_\infty$ . Before proceeding in this direction, we will first establish the following auxiliary lemma:

**Lemma 3.** For any vectors  $\mathbf{s} \in \mathbb{R}^{+p}$ ,  $\mathbf{x} \in \mathbb{R}^p$  and  $a_{l,m} \in \{0, 1\}$ , we have

$$\sum_{l=1}^n s_l \left( \sum_{m=1}^p a_{l,m} x_m \right)^2 \leq \max_{m \in \{1, 2, \dots, p\}} \left( \sum_{l=1}^n s_l a_{l,m} \right) \|\mathbf{x}\|_1^2. \blacksquare \quad (37)$$

**Proof.** We can assume without loss of generality that  $x_i \geq 0$  for all  $i \in \{1, 2, \dots, p\}$ , since if this were not true, we could always find an index  $i$  with  $x_i < 0$ , whereupon the transformation  $x_i \rightarrow -x_i$  would increase the LHS but keep the RHS the same. A series of such transformations can always lead us to an inequality where all elements of  $x_i$  are non-negative, which is stronger than the original result (and is proved here). Let  $k$  be the index defined as

$$k \equiv \arg \max_m \sum_{l=1}^n s_l a_{l,m} = \arg \max_m \sum_{l: a_{l,m}=1} s_l$$



In other words, the index  $k$  maximizes the sum of  $s_l$ 's chosen by the position of 1's in the column  $k$ . Then, note that for any two indices  $u, v$ , we have

$$\sum_{l=1}^n s_l a_{l,k} \geq \sum_{u: a_{l,u}=1} s_l \geq \sum_{\substack{u,v: a_{l,u}=1 \\ a_{l,v}=1}} s_l = \sum_{l=1}^n s_l a_{l,u} a_{l,v}$$

Following from this and the definition of  $k$  we have,

$$\begin{aligned} \max_{m \in \{1, 2, \dots, p\}} \left( \sum_{l=1}^n s_l a_{l,m} \right) \|\mathbf{x}\|_1^2 &= \left( \sum_{l=1}^n s_l a_{l,k} \right) \cdot \left( \sum_{u=1}^p x_u \right) \cdot \left( \sum_{v=1}^p x_v \right) \\ &= \sum_{\substack{l \in \{1, 2, \dots, n\} \\ u, v \in \{1, 2, \dots, p\}}} s_l a_{l,k} x_u x_v \\ &\geq \sum_{\substack{l \in \{1, 2, \dots, n\} \\ u, v \in \{1, 2, \dots, p\}}} s_l a_{l,u} x_u a_{l,v} x_v \\ &= \sum_{l=1}^n s_l \left( \sum_{m=1}^p a_{l,m} x_m \right)^2 \end{aligned}$$

as claimed. ■

From Equation 22, we have:

$$\mathbb{P} \left( |t_{1,k}| \geq \kappa \sqrt{2\theta \bar{\mathbf{R}}_k^T(\mathbf{A}\mathbf{x}^*)_2} \right) \leq 2e^{-\theta}. \quad (38)$$

The RHS involves a signal-dependent term  $\bar{\mathbf{R}}_k^T(\mathbf{A}\mathbf{x}^*)_2$ . We want to upper bound this quantity, independent of  $k$ , to obtain a concentration bound on  $\|\mathbf{t}_1\|_\infty$ :

$$\begin{aligned} \bar{\mathbf{R}}_k^T(\mathbf{A}\mathbf{x}^*)_2 &= \sum_{l=1}^n r_{k,l}^2 \left( \sum_{m=1}^p a_{l,m} x_m^* \right)^2 \\ &\leq \max_{\substack{k=1, \dots, p \\ m=1, \dots, p}} \left( \sum_{l=1}^n r_{k,l}^2 a_{l,m} \right) \|\mathbf{x}^*\|_1^2 \quad \text{using Lemma 3 with } s_k := r_{k,l}^2 \\ &= \|\mathbf{x}^*\|_1^2 W, \end{aligned} \quad (39)$$

where  $W := \max_{\substack{k=1, \dots, p \\ m=1, \dots, p}} \left( \sum_{l=1}^n r_{k,l}^2 a_{l,m} \right) = \max_{\substack{k=1, \dots, p \\ m=1, \dots, p}} \left( (\bar{\mathbf{R}}^T \mathbf{A})_{k,m} \right)$ .

From Equation (38) and Equation (39) we have, with probability  $\geq 1 - 2pe^{-\theta}$ ,

$$\|\mathbf{t}_1\|_\infty \leq \kappa \sqrt{2\theta \|\mathbf{x}^*\|_1^2 W}. \quad (40)$$

The probability  $1 - 2pe^{-\theta}$  is obtained from a union bound. However, the quantity  $\|\mathbf{x}^*\|_1$  is still unknown. We need to derive an estimator for  $\|\mathbf{x}^*\|_1$  to bound  $\|\mathbf{t}_1\|_\infty$  in computable terms.

### 3.4. Estimating $\|\mathbf{x}^*\|_1$

As mentioned in the discussions of both Equation (40) and Lemma 1, to obtain an input signal independent upper bound on  $\|\mathbf{t}_1\|_\infty$  and  $\|\mathbf{t}_2\|_\infty$ , we need to derive an estimator which presents theoretical guarantees for the upper bound of  $\|\mathbf{x}^*\|_1$ . Instead of a direct upper bound, it is much easier to set a bound on  $\sum_{l,k} a_{l,k} x_k^*$  (recall that all elements of  $\mathbf{x}^*$  are non-negative) and invoke a second inequality to obtain the concentration bound on  $\|\mathbf{x}^*\|_1$ . With this in mind, since  $\mathbf{A}$  is a Bernoulli Sensing Matrix with a parameter  $q$ , we can invoke Bernstein's inequality. To make the paper self-contained, we state Bernstein's inequality from [3] for our case of Bernoulli random variables here below as Lemma 4.

**Lemma 4. (Bernstein Inequality)** *Let  $X_1, \dots, X_n$  be independent zero-mean random variables. Suppose that  $|X_i| \leq M$  for all  $i$ , then for all positive  $t$ , we have*

$$\mathbb{P} \left( \sum_{i=1}^n X_i \geq t \right) = \mathbb{P} \left( \sum_{i=1}^n X_i \leq -t \right) \leq \exp \left( - \frac{\frac{1}{2}t^2}{\sum_{i=1}^n \mathbb{E}[X_i^2] + \frac{1}{3}Mt} \right). \quad (41)$$

We adapt this to our case of Bernoulli random variables. Let  $S_n := \sum_{i=1}^n X_i$  where  $X_i \sim \text{Ber}(q)$ . Then,

$$\mathbb{P} \left( S_n \leq nq - \frac{\theta}{3} \max(q, 1-q) - \sqrt{2\theta nq(1-q)} \right) \leq e^{-\theta}. \blacksquare \quad (42)$$

**Proof:** To apply Bernstein inequality, we first center  $X_i \leftarrow X_i - \mathbb{E}[X_i]$ . Then, we have

$$|X_i - \mathbb{E}[X_i]| = |X_i - q| \leq \max(q, 1-q) \quad \text{and} \quad \sum_{i=1}^n \mathbb{E}[X_i^2] = nq(1-q).$$

Invoking Equation (41) we can state,

$$\mathbb{P}(S_n - nq \leq -t) \leq \exp\left(-\frac{t^2/2}{\frac{t}{3}\max(q, 1-q) + nq(1-q)}\right). \quad (43)$$

Let us define  $\theta := \frac{t^2/2}{\frac{t}{3}\max(q, 1-q) + nq(1-q)}$ . Rewriting,

$$\begin{aligned} t &= \frac{\theta}{3}\max(q, 1-q) + \sqrt{\frac{\theta^2(\max(q, 1-q))^2}{9} + 2\theta nq(1-q)} \\ &\geq \frac{\theta}{3}\max(q, 1-q) + \sqrt{2\theta nq(1-q)}. \end{aligned}$$

Hence, this inequality combined with Equation (43) gives us the required statement in Equation (42). ■

Since  $a_{l,k}$  are i.i.d. Bernoulli random variables, such that  $a_{l,k} \sim \text{Ber}(q)$ , we can utilise Lemma 4 with  $X_l = a_{l,k}$  where  $l \in \{1, \dots, n\}$ . Therefore for any given  $k = 1, \dots, p$ , we have with probability larger than  $1 - e^{-\theta}$ :

$$\sum_{l=1}^n (a_{l,k} - q) \geq -C_{n,\theta} \quad \text{where} \quad C_{n,\theta} := \sqrt{2nq(1-q)\theta} + \max(q, 1-q)\frac{\theta}{3}. \quad (44)$$

Hence on the same event for any given  $k$  we have:

$$nq - C_{n,\theta} \leq \sum_{l=1}^n a_{l,k} = \mathbf{1}_{1 \times n} \mathbf{A}_k \implies (nq - C_{n,\theta}) \mathbf{x}_k^* \leq \mathbf{1}_{1 \times n} \mathbf{A}_k \mathbf{x}_k^*.$$

Summing over  $k = 1, \dots, p$  we have the following expression:

$$(nq - C_{n,\theta}) \|\mathbf{x}^*\|_1 \leq \bar{x}_a \quad \text{where} \quad \bar{x}_a = \sum_{l,k} a_{l,k} \mathbf{x}_k^* = \mathbf{1}_{1 \times n} \mathbf{A} \mathbf{x}^*, \quad (45)$$

which holds with probability  $\geq (1 - e^{-\theta})^p$ , since the columns  $\mathbf{A}_k$  are mutually independent. Now since  $p \geq 1$  and  $e^{-\theta} < 1$ , we can state  $(1 - e^{-\theta})^p \geq 1 - pe^{-\theta}$  via Bernoulli's inequality [4]. For simplicity we consider Equation (45) to be true with probability  $\geq 1 - pe^{-\theta}$ .

The first assumption on the range of  $(n, q)$  is to assume that  $nq > C_{n,\theta}$ , which is implied by

$$nq \geq 4 \max(q, 1-q)\theta. \quad (46)$$

from a similar argument as presented in Comment 3 of the discussion following Proposition 1 and Proposition 2.

Now, to obtain an upper bound on  $\|\mathbf{x}^*\|_1$ , we need to find some concentration bound on  $\bar{x}_a$ . We bound  $\mathbf{1}_{n \times 1} \mathbf{A} \mathbf{x}^*$  using Lemma 2. Setting  $\mathbf{R} = -\mathbf{1}_{n \times 1}$  in Equation (34), we have with probability  $\geq 1 - 2e^{-\theta}$ :

$$\underbrace{\mathbf{1}_{1 \times n} \mathbf{A} \mathbf{x}^*}_{\bar{x}_a} < \sum_{i=1}^n y_i + \sqrt{\sum_{i=1}^n y_i^2 \frac{\kappa \sqrt{2\theta}}{1 - \kappa \sqrt{2g(\theta)}}}. \quad (47)$$

In this case with probability  $\geq 1 - (p + 2)e^{-\theta}$

$$\|\mathbf{x}^*\|_1 \leq \frac{1}{nq - C_{n,\theta}} \left( \sum_{i=1}^n y_i + \sqrt{\sum_{i=1}^n y_i^2 \frac{\kappa \sqrt{2\theta}}{1 - \kappa \sqrt{2g(\theta)}}} \right) := \hat{\Lambda}_\theta. \quad (48)$$

Note that  $\hat{\Lambda}$  in Proposition 1 is obtained from  $\hat{\Lambda}_\theta$  defined above by setting  $\theta := 3 \ln p$ . We show a numerical illustration of the expression for  $\hat{\Lambda}$  on over 1000 simulations in the section on numerical experiments in the main paper (Figure 4). Now that we have the required estimator  $\hat{\Lambda}$  for  $\|\mathbf{x}^*\|_1$ , we can use it in Equation (40) to obtain the required bound on  $\|\mathbf{t}_1\|_\infty$ . With probability  $\geq 1 - (3p + 2)e^{-\theta}$ , we have:

$$\|\mathbf{t}_1\|_\infty \leq \kappa \hat{\Lambda}_\theta \sqrt{2\theta W} \quad (49)$$

Further combining Lemma 1 and Equation (48) along with their underlying assumptions, we state the required upper bound on  $\|\mathbf{t}_2\|_\infty$  in the following Lemma 5.

**Lemma 5.** *Let there exist some positive constants  $c_2$  and  $c_3$  such that as soon as  $n \geq 2$  and  $\theta > 1$ , with probability larger than  $1 - c_3 p^2 e^{-\theta}$*

$$\|\mathbf{t}_2\|_\infty \leq c_2 \left( \frac{\theta}{n} + \frac{\max(q^2, (1-q)^2)}{n^2 q (1-q)} \theta^2 \right) \hat{\Lambda}_\theta, \quad (50)$$

where

$$\hat{\Lambda}_\theta := \frac{1}{nq - C_{n,\theta}} \left( \sum_{i=1}^n y_i + \sqrt{\sum_{i=1}^n y_i^2 \frac{\kappa \sqrt{2\theta}}{1 - \kappa \sqrt{2g(\theta)}}} \right),$$

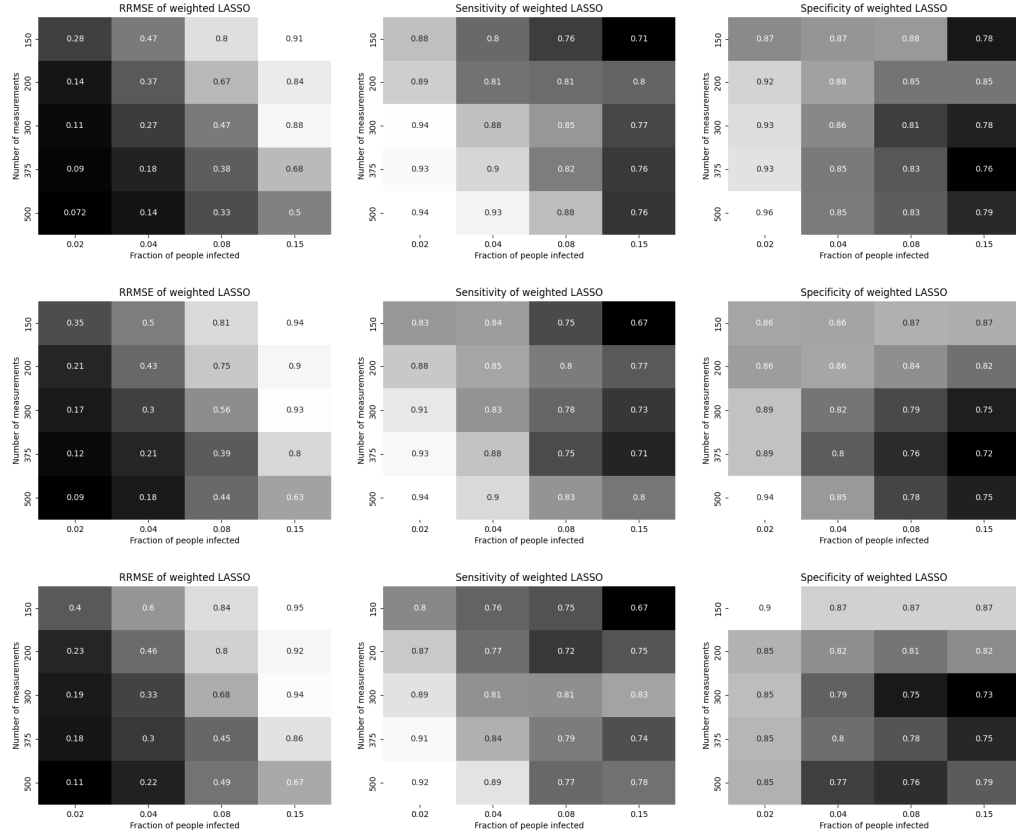


Figure 1: RRMSE, Sensitivity and Specificity values for  $\sigma \in \{0.1, 0.15, 0.2\}$  (top to bottom), versus the number of measurements  $n$  and  $f_s$  (fraction of people infected out of a total of  $p$ ). The results are for the WLASSO algorithm. Lower is better for RRMSE, and higher is better for the rest.

and

$$C_{n,\theta} = \sqrt{2nq(1-q)\theta} + \max(q, 1-q)\frac{\theta}{3},$$

under the assumption  $nq \geq 4 \max(q, 1-q)\theta$ .

**Note:** Equation (49) combined with Lemma 5 for  $\|\mathbf{t}_2\|_\infty$  produces the constant weight stated in Proposition 1. On the other hand, Equation (36) combined with Lemma 5 leads to Proposition 2. In both cases, we set  $\theta := 3 \ln p$  which gives us bounds having high probability  $\geq 1 - \frac{c'}{p}$ .

#### 4. Additional Numerical Results

We present some additional numerical results for the same experimental setup and parameters as in the main paper, except that we select  $\sigma \in \{0.1, 0.15, 0.2\}$  over and above the experiment with  $\sigma = 0.05$  in the main paper. Here  $\sigma$  is the standard deviation of the Gaussian noise on noting cycle time values in RT-PCR. These results (RRMSE, sensitivity, specificity) are shown in Fig. 1. The general trend of performance improving with increase in  $n$  or decrease in  $\ell_0$  norm ( $= f_s p$ ) are visible in these plots as well. Note that values of  $\sigma$  higher than 0.2 are neither physically realistic nor would they satisfy Assumption A3 of Proposition 1 of the main paper. Hence we did not further experiment with them.

#### References

- [1] S. Negahban, P. Ravikumar, M. J. Wainwright, B. Yu, A unified framework for high-dimensional analysis of M-estimators with decomposable regularizers, *Statistical Science* 27 (4) (2012) 538–557.
- [2] X. J. Hunt, P. Reynaud-Bouret, V. Rivoirard, L. Sansonnet, R. Willett, A data-dependent weighted LASSO under Poisson noise, *IEEE Transactions on Information Theory* 65 (3) (2018) 1589–1613. doi:10.1109/TIT.2018.2869578.
- [3] Bernstein inequalities (probability theory), [https://en.wikipedia.org/wiki/Bernstein\\_inequalities\\_\(probability\\_theory\)](https://en.wikipedia.org/wiki/Bernstein_inequalities_(probability_theory)).
- [4] Bernoulli's inequality, [https://en.wikipedia.org/wiki/Bernoulli's\\_inequality](https://en.wikipedia.org/wiki/Bernoulli's_inequality).